Chapter IV

EXPERIMENTAL RESULTS

The experimental results are divided into two parts. The first part deals with some hydrodynamic properties of the fluidized-bed column. The second parts, deals with studying mass transfer coefficient of ammonia gas.

4.1 Experimental Results in Studying Hydrodynamic Properties of the Fluidized-bed Column

4.1.1 Dependence of Hydraulic Resistance of Bed on Superficial Gas Velocity

Effects of gas velocity on hydraulic resistance of bed were studied. The results are shown in Figure 4.1 and 4.2. It has been observed that at superficial gas velocity lower than about 110 cm/sec. there is a sharp increase in hydraulic resistance of bed. But at gas velocity higher than 110 cm/sec, there is almost no variation of pressure drop with gas velocity in the range of gas velocities studying.

4.1.2 Dependence of Hydraulic Resistance of Bed on Superficial Liquid Velocity

At gas velocity 283 cm/sec. four values of liquid velocity

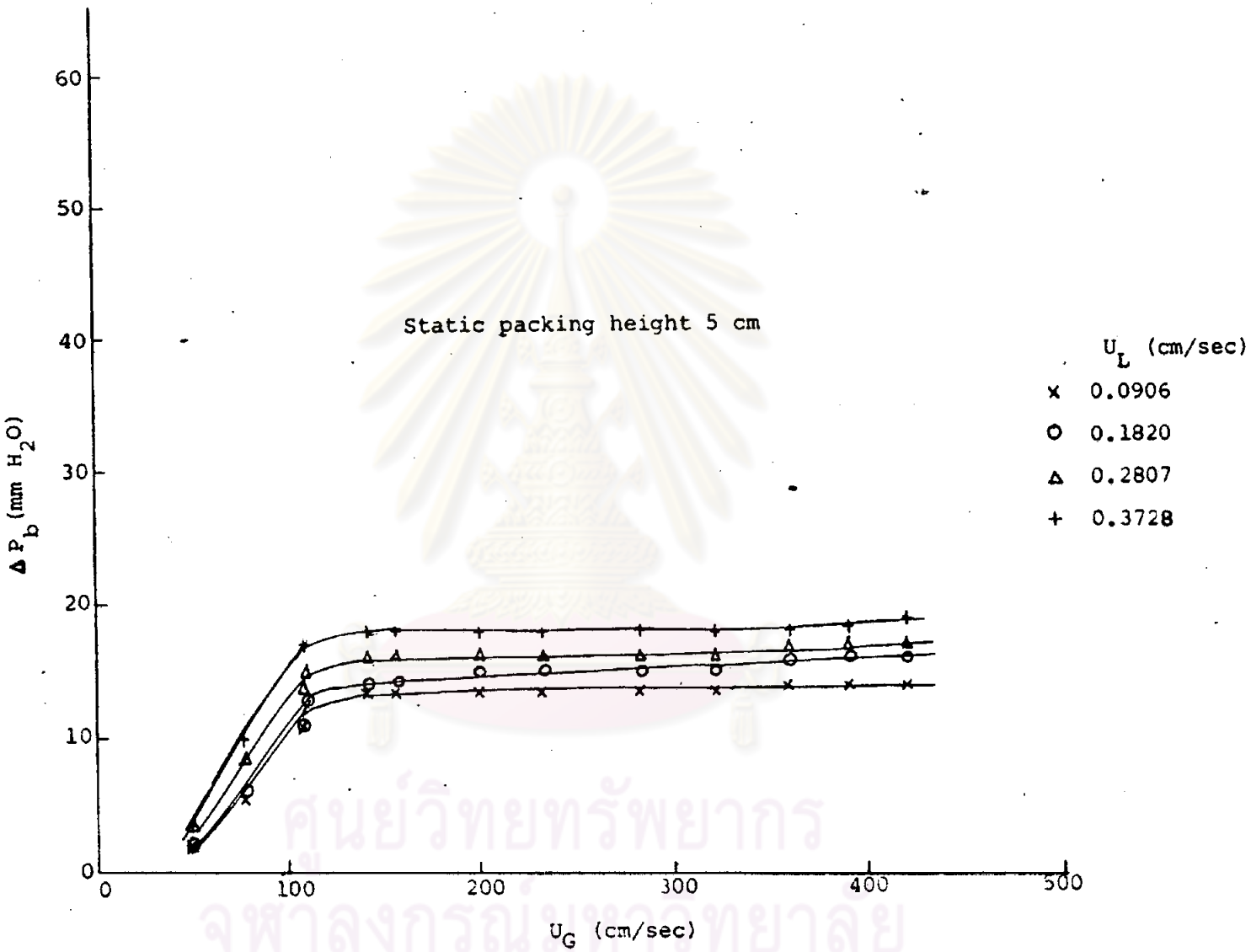

Fig.4.1 Variation of superficial gas velocity on hydraulic resistance of bed at static packing height 5 cm

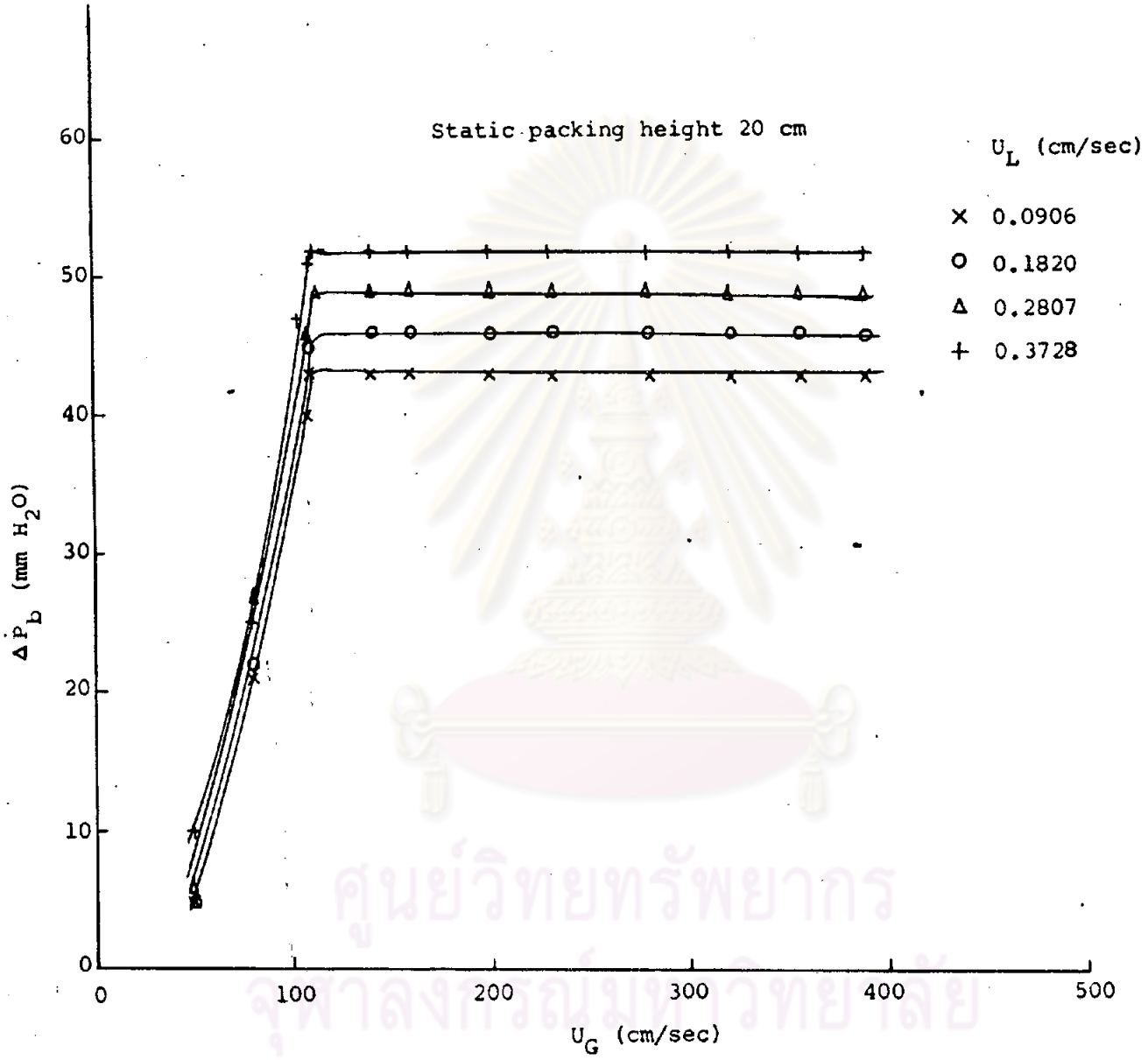

Fig.4.2 Variation of superficial gas velocity on hydraulic resistance of bed at static pasking height 20 cm

were used to study the effect of superficial liquid velocity on hydraulic resistance of bed. The results are shown in Table C-3 and plotted in Figure 4.3. It was observed that hydraulic resistance of bed increased with increasing bed height.

4.1.3 Dependence of Hydraulic Resistance of Bed on Static Packing Height

Four values of static bed height 5, 10, 15 and 20 cm. were used at constant superficial gas velocity 283 cm/sec. The results are shown in Table C-4 and plotted in Figure 4.4. The hydraulic resistance of bed also increased linearly with increasing bed height.

4.1.4 Minimum Fluidization Velocity.

The determination of minimum fluidization velocities were carried out through the measurement of bed height. Eight values of gas mass velocity between 0.167 to 0.495 $gm/cm^2 sec.$ were used at four constant bed height and four constant liquid velocities. It was observed that the aerated bed height were varied linearly with gas mass velocities for any particular set of liquid mass velocity and static packing height. The linear plot of aerated bed heights with gas mass velocities can be extrapolated to the point of bed height equal to the static bed height and the abscissa of this point, as shown in Figure 4.5-4.8 according to the definition of minimum fluidization velocity

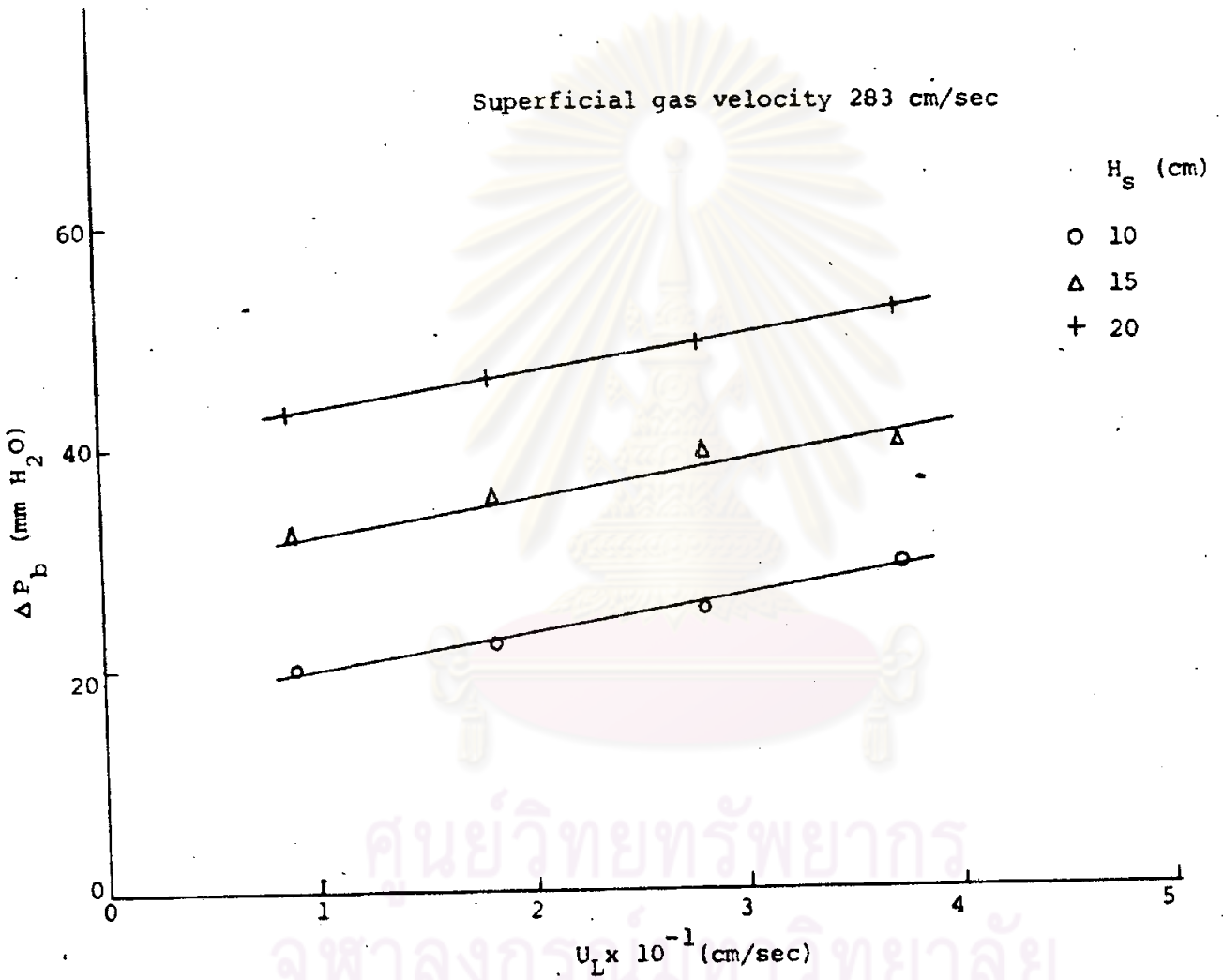

Fig.4.3 Variation of superficial liquid velocity on hydraulic resistance of bed at superficial gas velocity 283 cm/sec

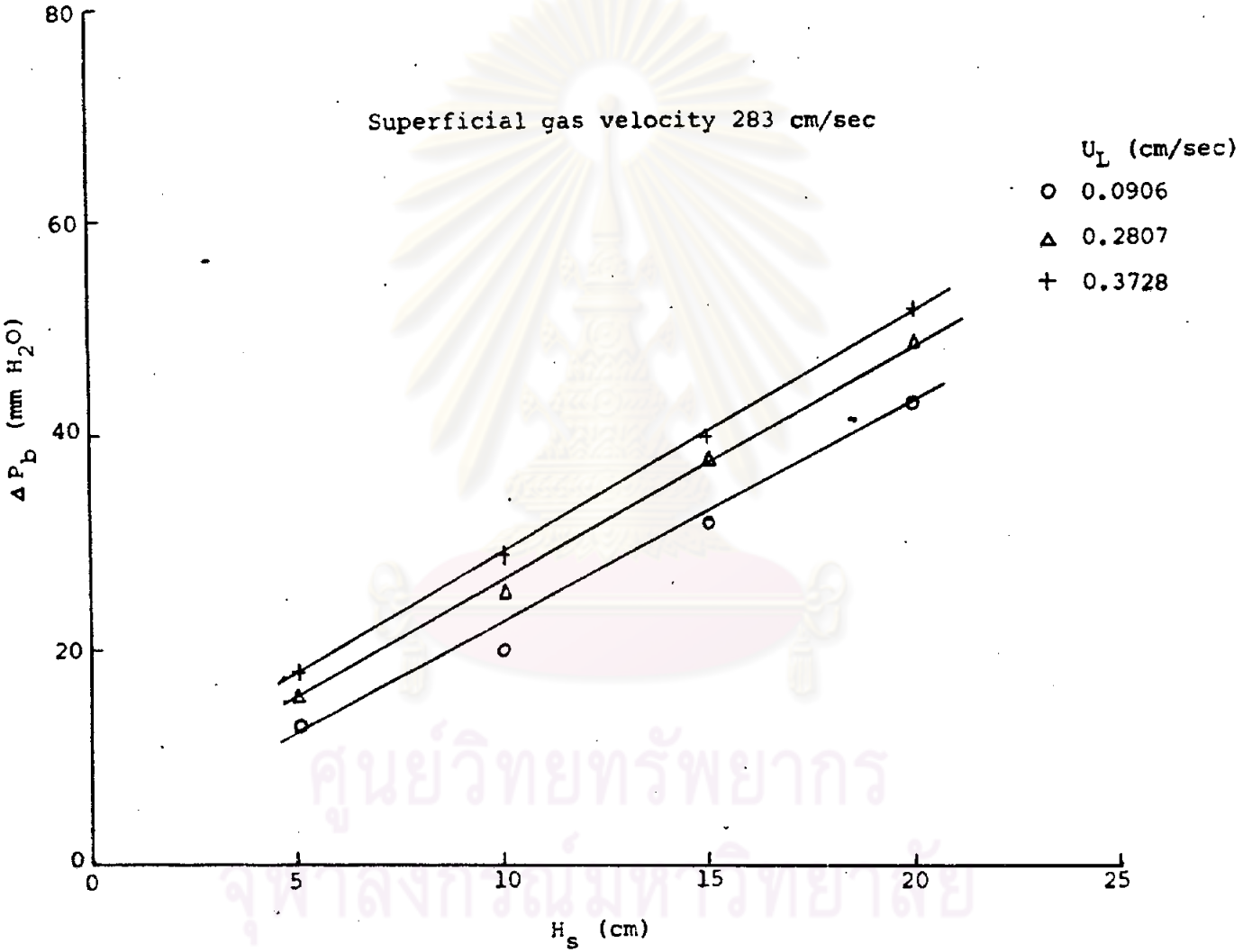

Fig.4.4 Variation of static bed height on hydraulic resistance of bed at superficial gas velocity 283 cm/sec

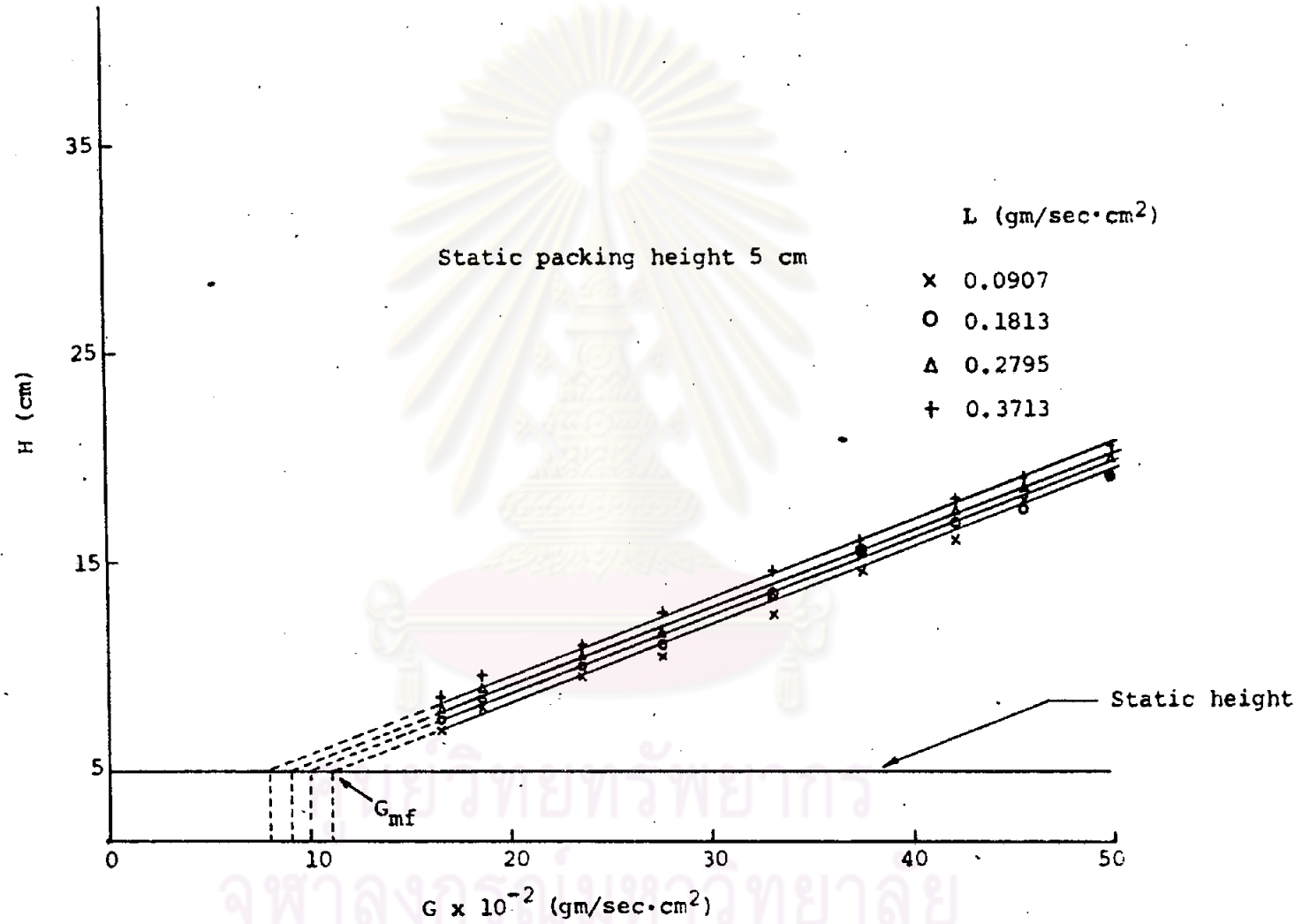

Fig.4.5 Determination of minimum fluidization velocity from bed height at static bed height 5 cm

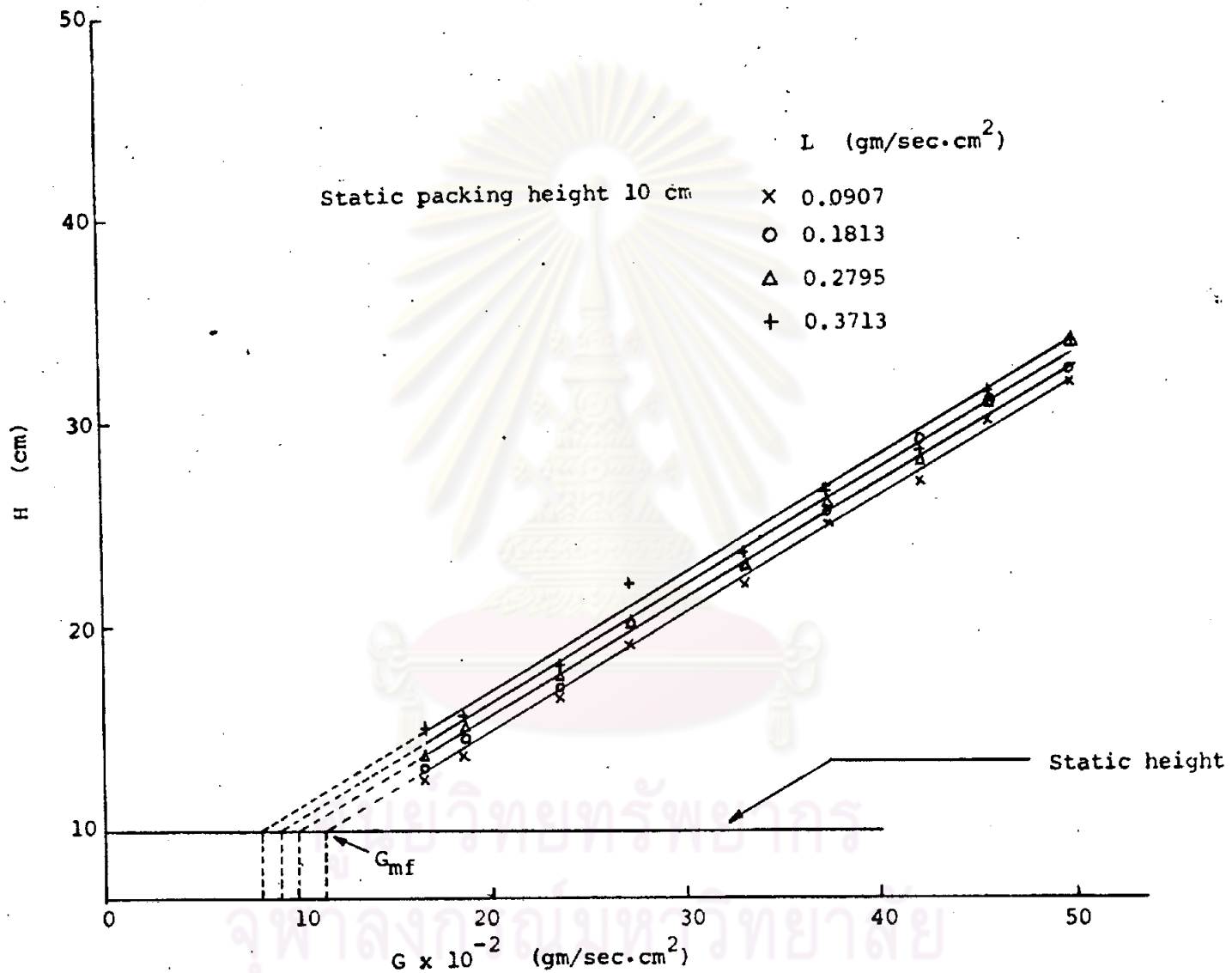

Fig.4.6 Determination of minimum fluidization velocity from bed height at static bed height 10 cm

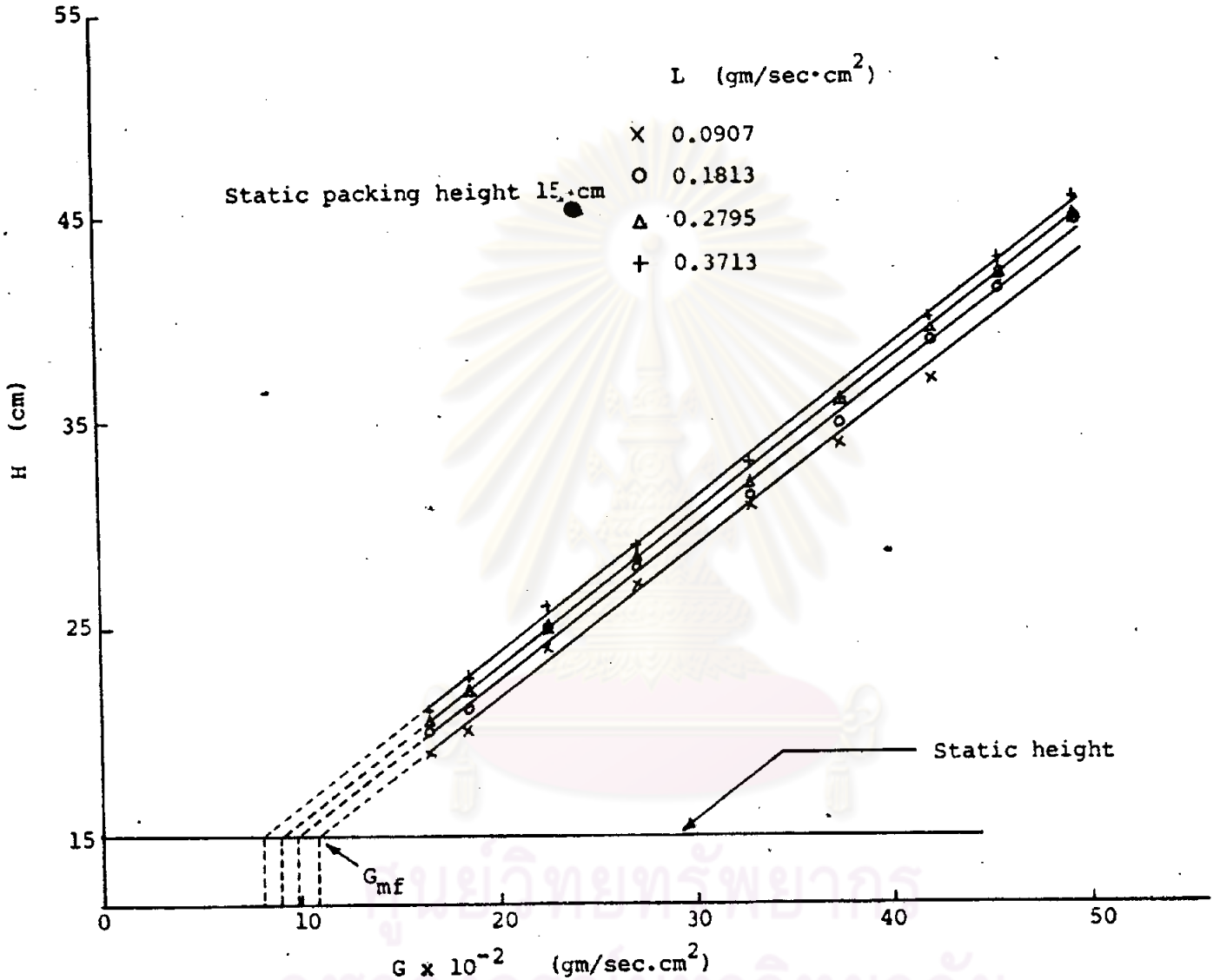

Fig.4.7 Determination of minimum fluidization velocity from bed height at static bed height 15 cm

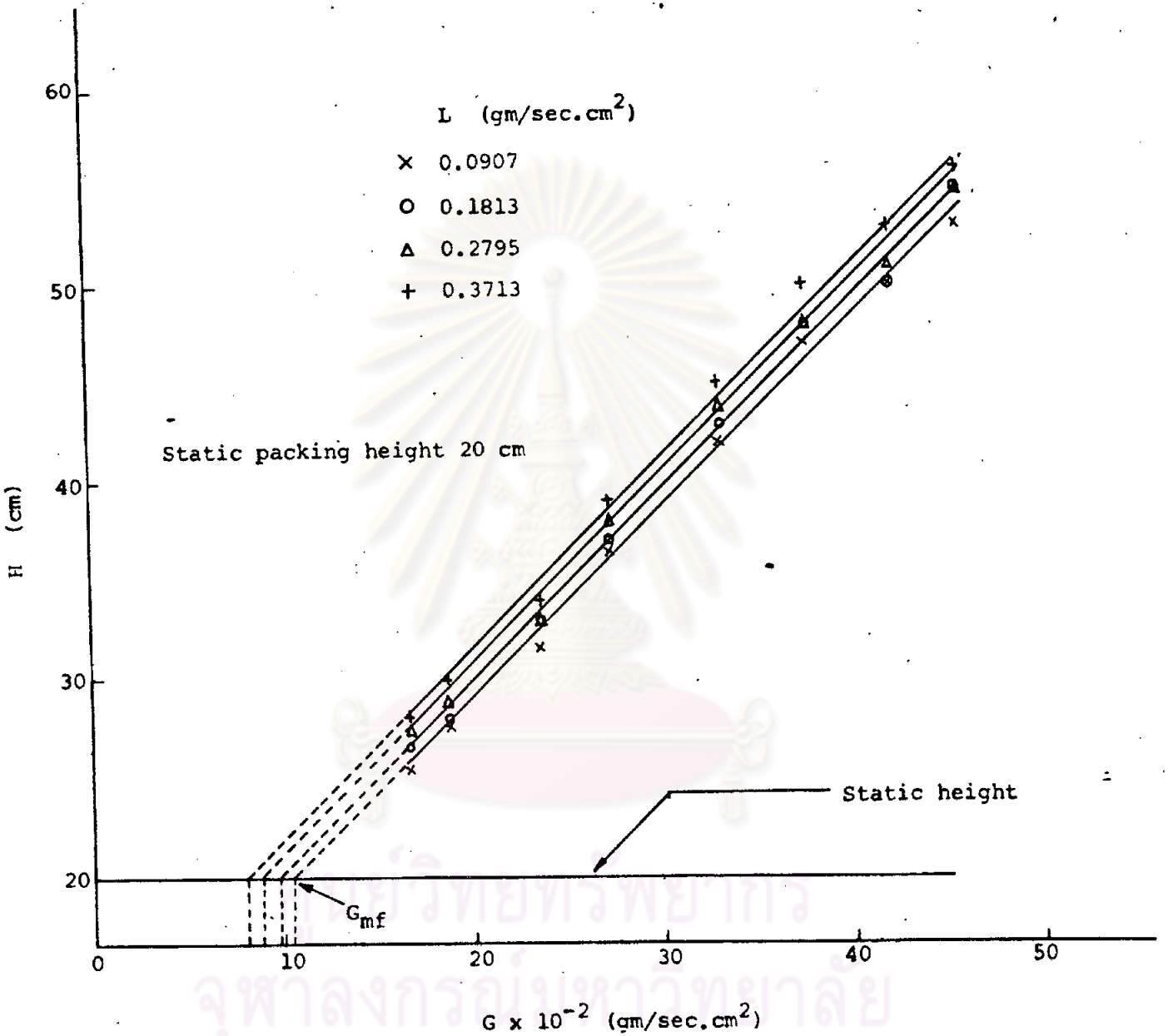

Fig.4.8 Determination of minimum fluidization velocity from bed height at static bed height 20 cm

for the experimental condition used. The experimental data are shown in Table C-5 and plotted in Figure 4.5-4.8. The results are shown in Table C-6 and plotted in Figure 4.9. It was observed that the minimum fluidization velocities were not varied with static packing height and varied slightly with liquid mass velocities.

4.1.5 Effect of Superficial Gas Velocities, Liquid Velocities and Bed Heights on Gas Hold-up(ϵ_G) and Liquid Hold-up(ϵ_L)

Liquid velocities at 0.1820, 0.2807 and 0.3728 cm/sec were used at constant bed height 5, 10 and 20 cm. and constant gas velocities 157, 232, 283 and 390 cm/sec. The height of clear liquid at various liquid velocities, bed heights and gas velocities are shown in Table C-7. It seems to be no effect of gas velocity on height of clear liquid but height of clear liquid increased with increasing liquid velocity and static bed height. The results of gas holdup and liquid holdup are shown in Table C-8 and C-9. It was obserbed that ϵ_G were not effect by bed heights and liquid velocities but increased with increasing gas velocities. Liquid hold-up decreased as increasing gas velocities and bed height and increased with increasing liquid velocities.

4.2 Experimental Results in Studying Mass Transfer Coefficient ($K_G a$) of Ammonia Gas in Water

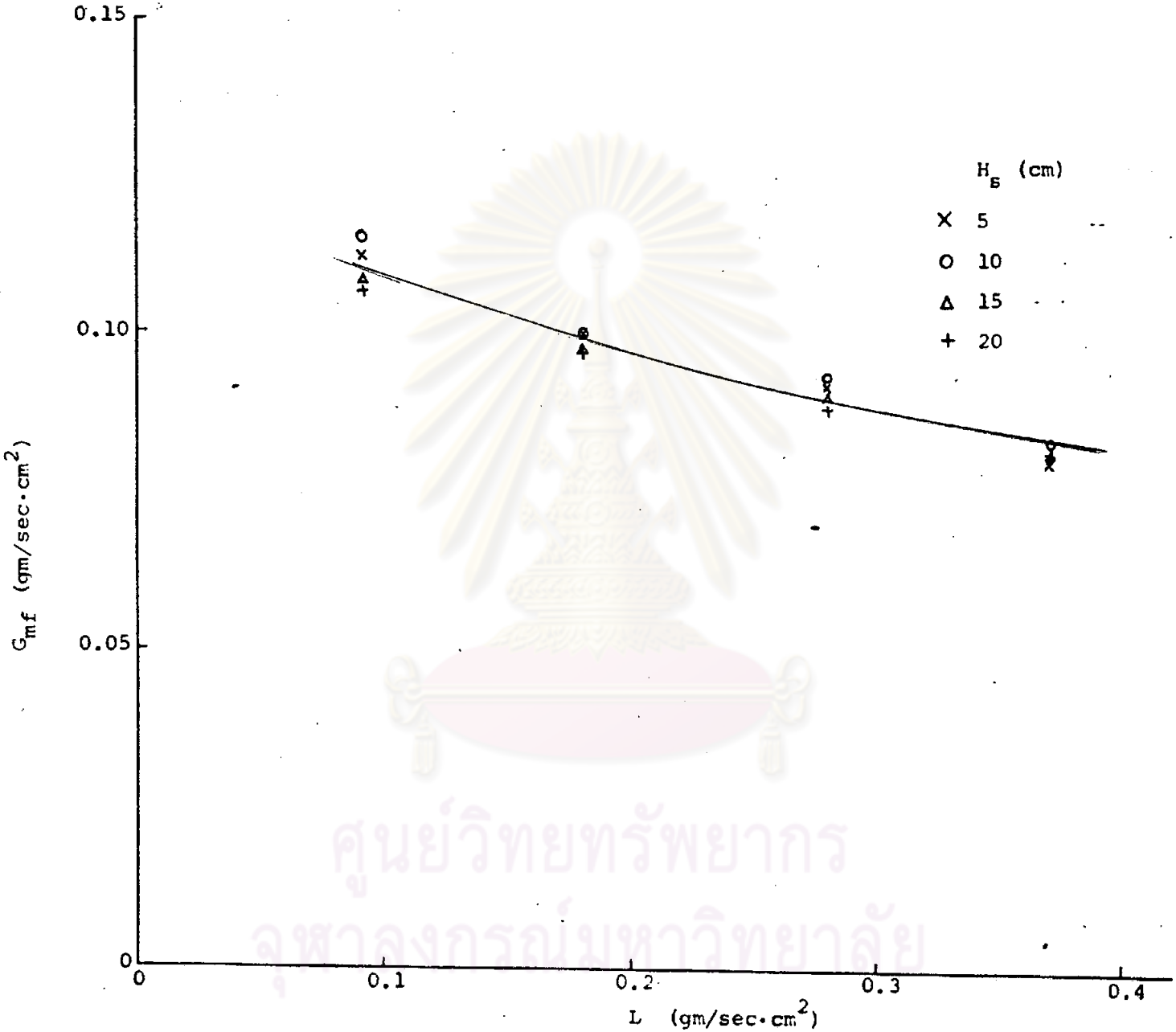

Fig.4.9 Variation of minimum fluidization velocity with liquid mass velocity

In order to investigate that gas absorption in a fluidized-bed column has higher efficiency and capacity for a given tower volume than common packed tower and to study the effects of liquid velocities, gas velocities and bed heights at various mole fraction of ammonia on mass transfer coefficient, the mass transfer coefficients were calculated and the results were compared with packed tower.

4.2.1 Effects of Gas Velocities on Mass Transfer Coefficient (K_Ga)

Five values of Gas velocity were used and Froude numbers were calculated and plotted with mass transfer coefficients. The results were shown in Table C-12, C-13 and plotted in Figure 4.10-4.17. It was observed that K_Ga increased with increasing gas velocity. The slope of each line was calculated by using least square method and the average value of the slope was 0.495.

4.2.2 Effects of Liquid Velocities on Mass Transfer Coefficient (K_Ga)

Five values of liquid velocity were used at constant bed height 8.9 cm. The Reynolds Number were calculated and plotted with K_Ga. The results were shown in Table C-14 and plotted in Figure 4.18-4.21. K_Ga also increased with increasing Reynolds number in the same manner as Froude number. The slope of the lines

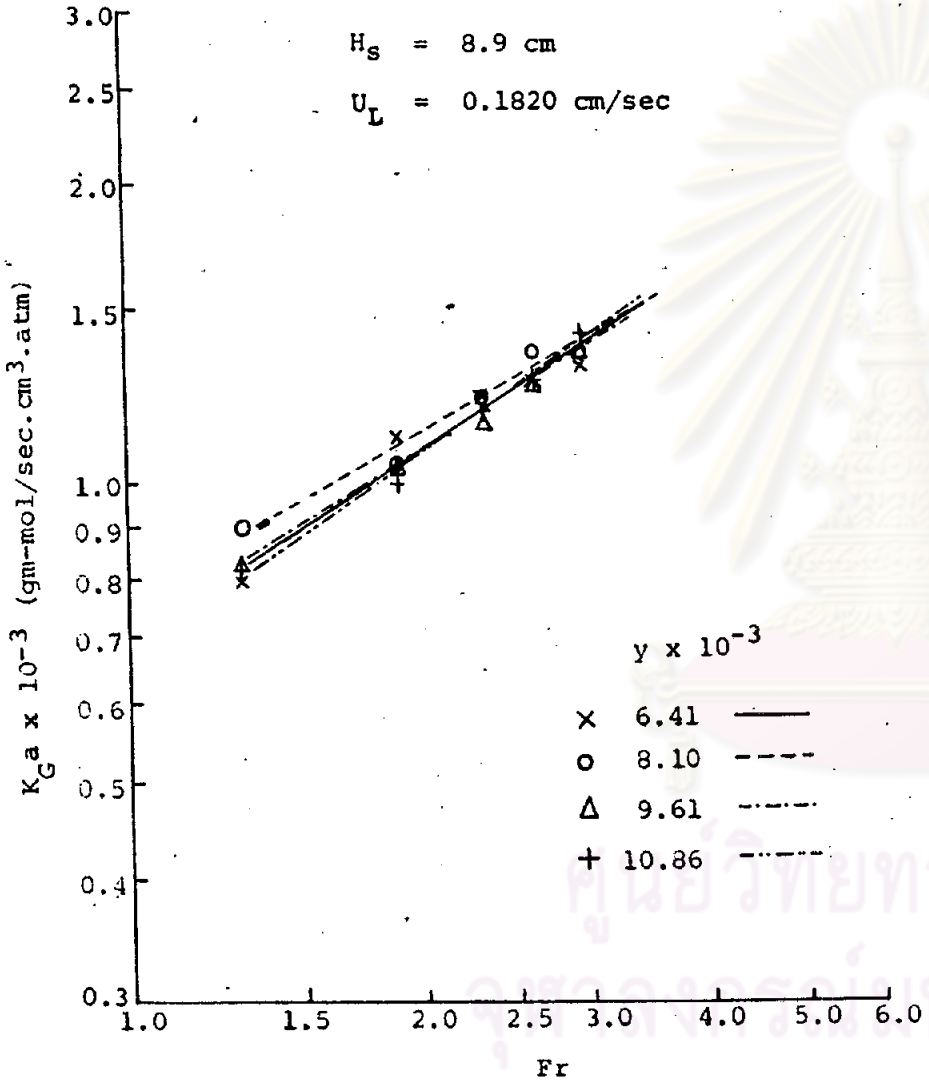

Fig.4.10 Variation of $K_G a$ with Fr at H_S = 8.9 cm, U_L = 0.1820 cm/sec

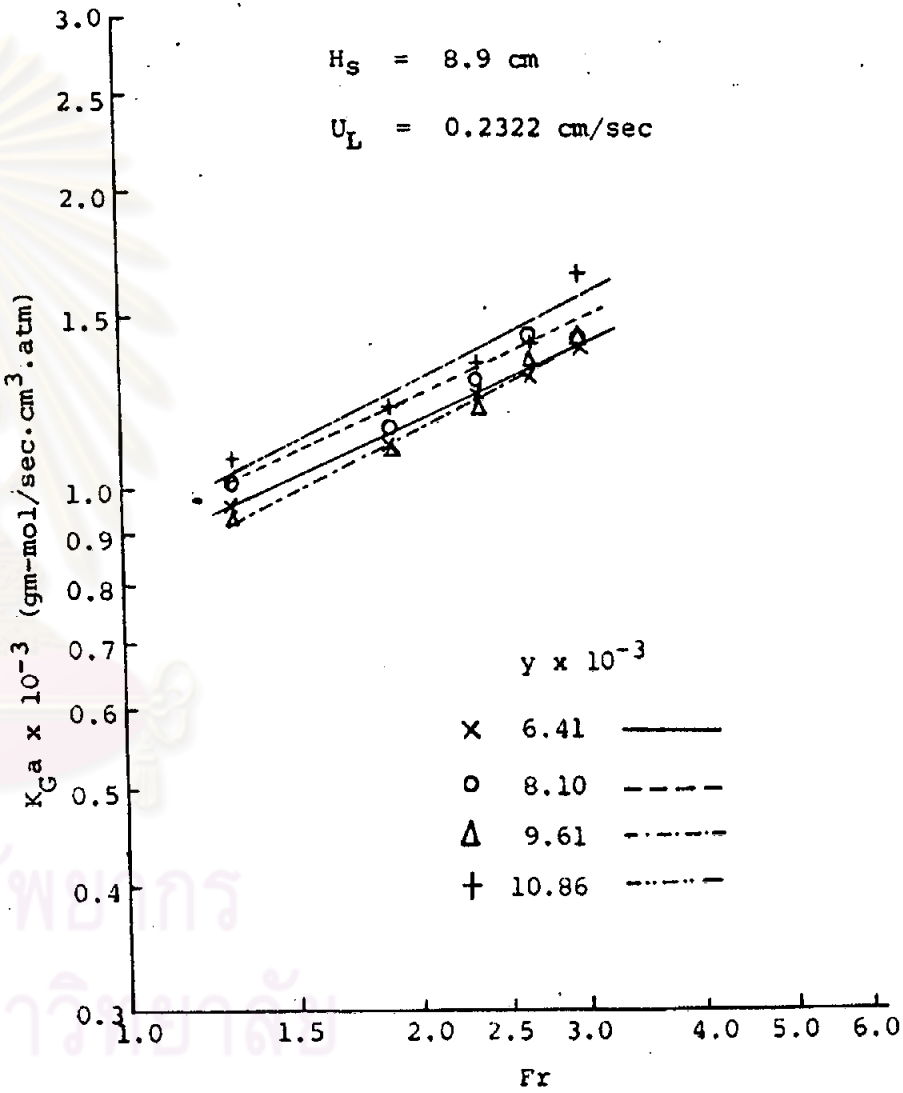

Fig.4.11 Variation of $K_G a$ with Fr at H_S = 8.9 cm, U_L = 0.2322 cm/sec

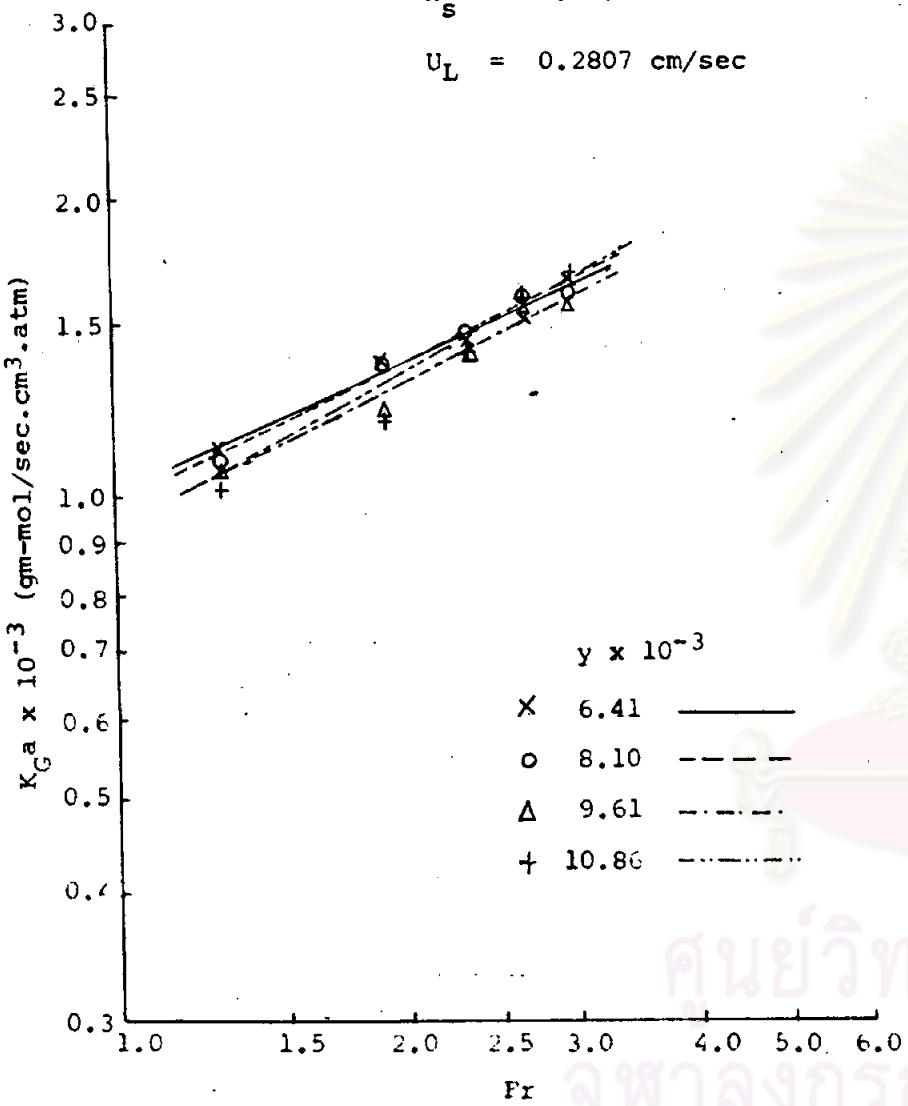

Fig.4.12 Variation of $K_G a$ with Fr at H_s = 8.9 cm

U_L = 0.2807 cm/sec

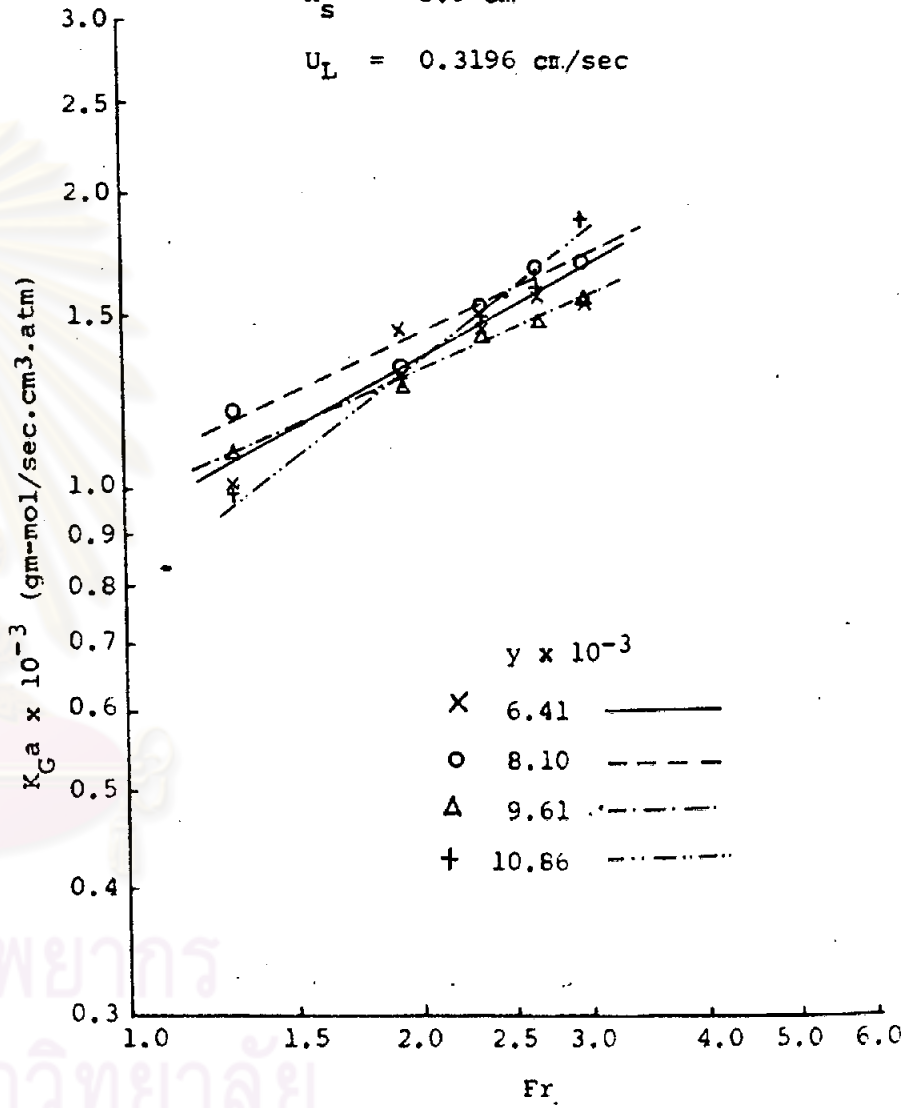

Fig.4.13 Variation of $K_G a$ with Fr at h_s = 8.9 cm

U_L = 0.3196 cm/sec

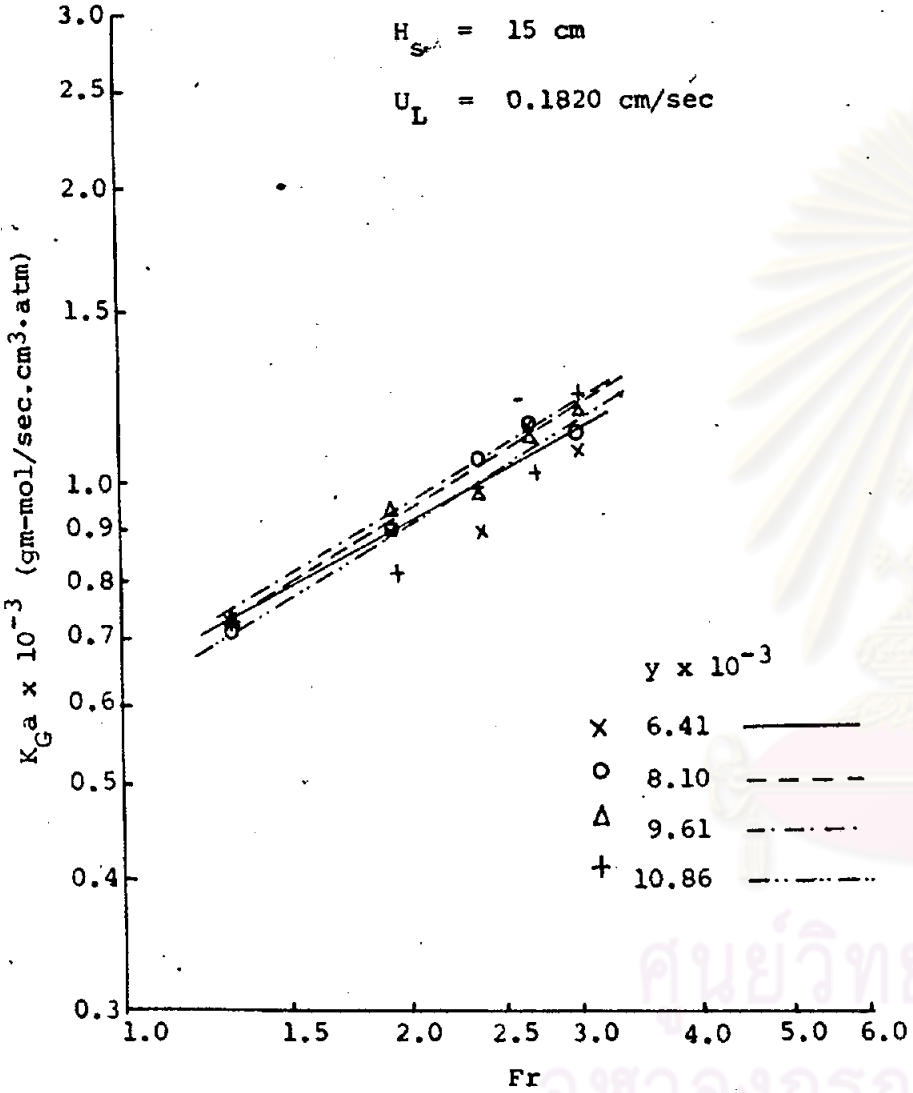

Fig.4.14 Variation of $K_G a$ with Fr at H_S = 15 cm,

U_L = 0.1820 cm/sec

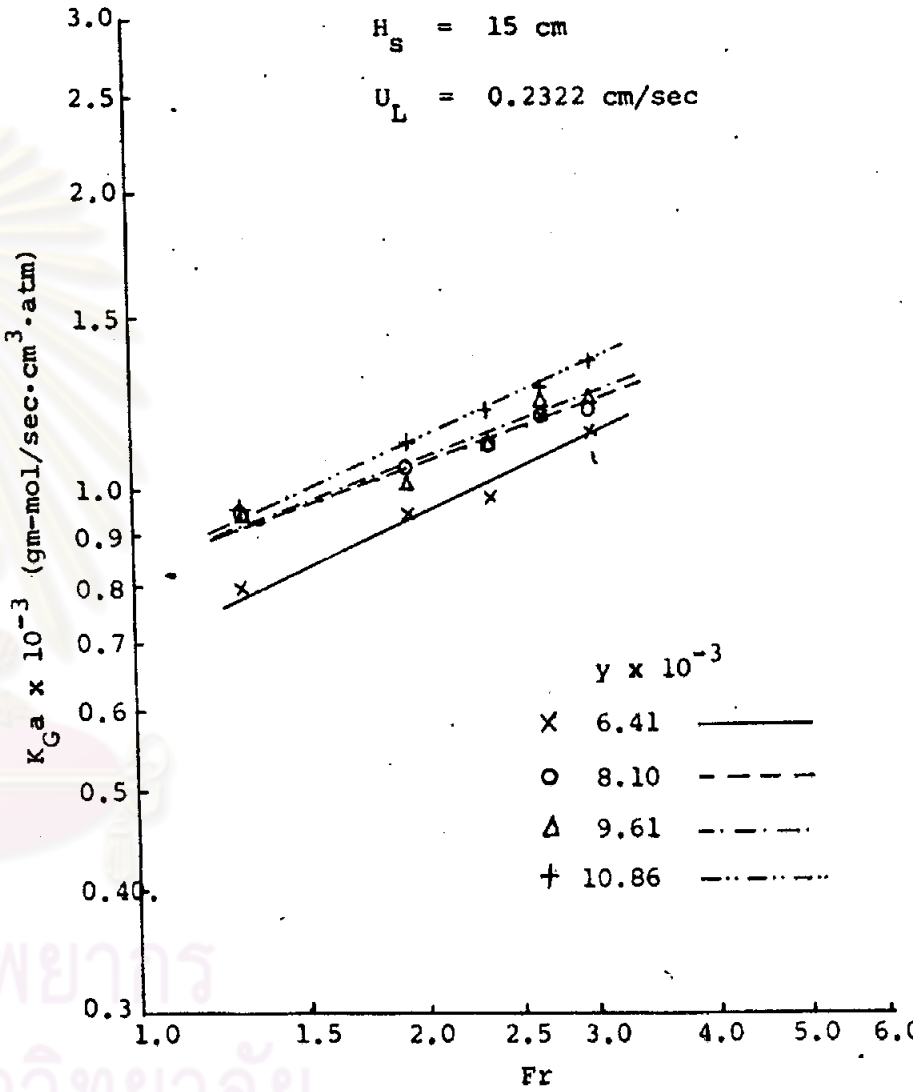

Fig.4.15 Variation of $K_G a$ with Fr at H_S = 15 cm

U_L = 0.2322 cm/sec

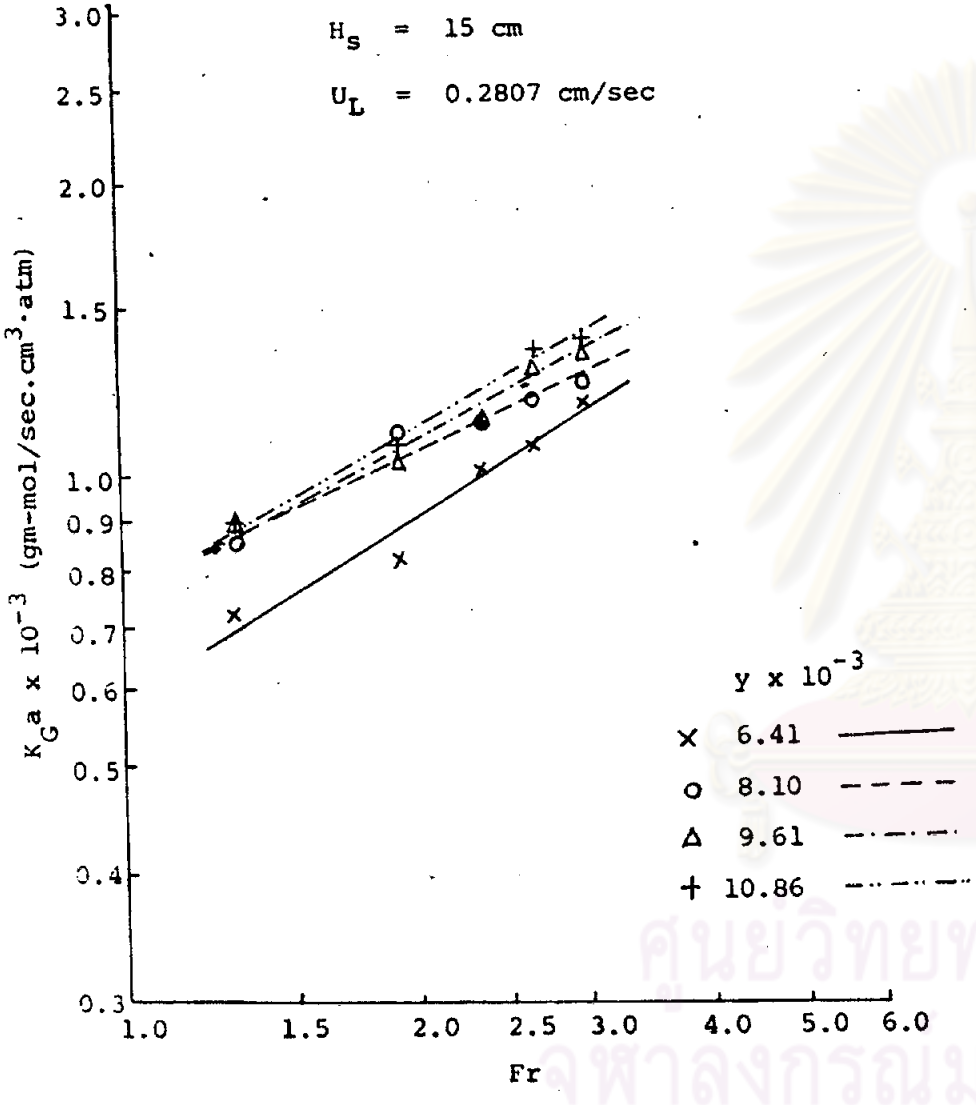

Fig.4.16 Variation of $K_G a$ with Fr at H_s = 15 cm, U_L = 0.2807 cm/sec

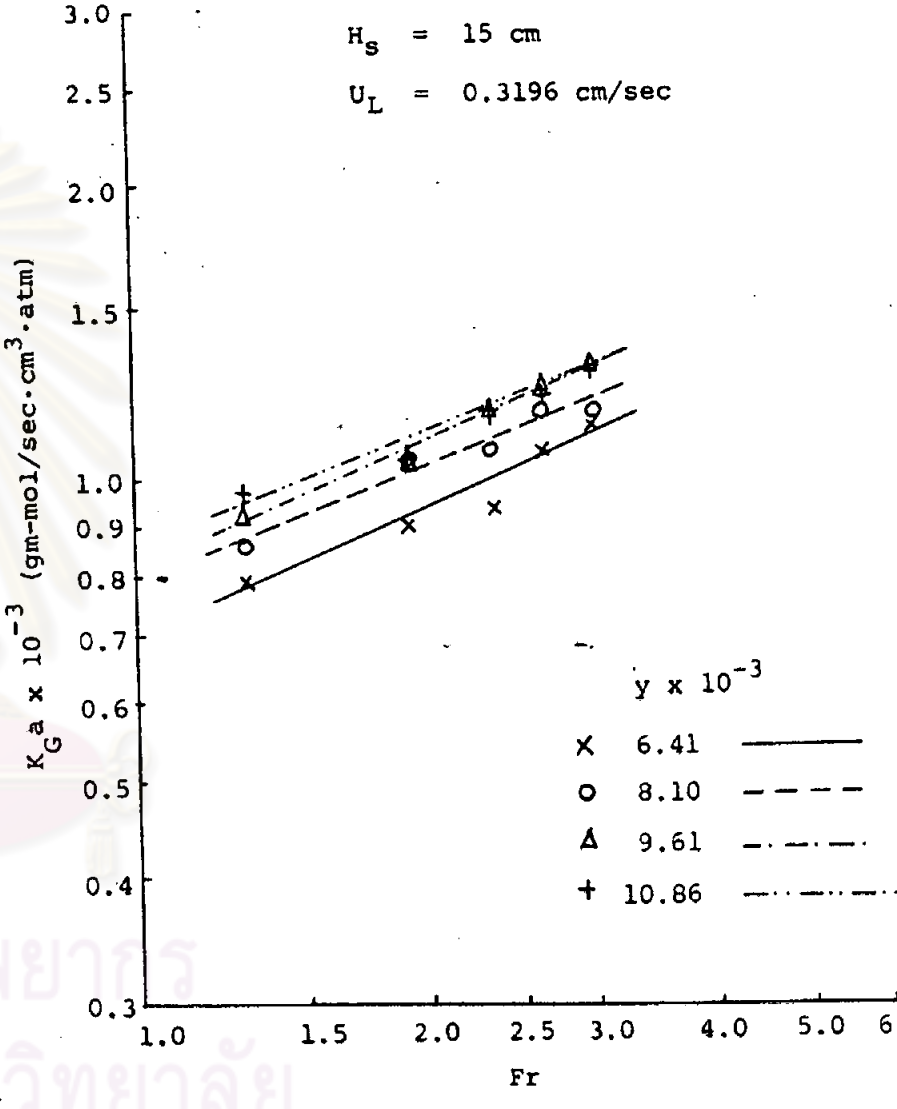

Fig.4.17 Variation of $K_G a$ with Fr at H_s = 15 U_L = 0.3196 cm/sec

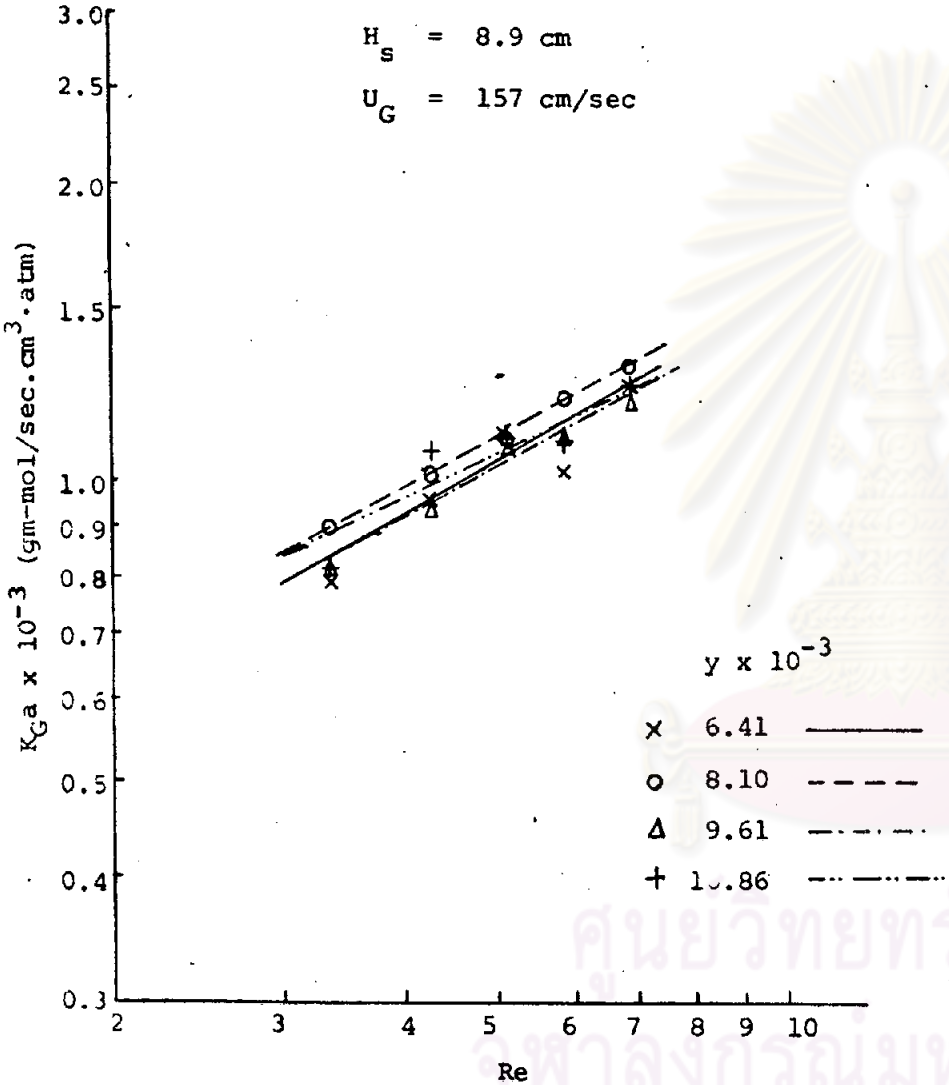

Fig.4.18 Variation of $K_G a$ with Re_L at H_s = 8.9 cm,

U_G = 157 cm/sec

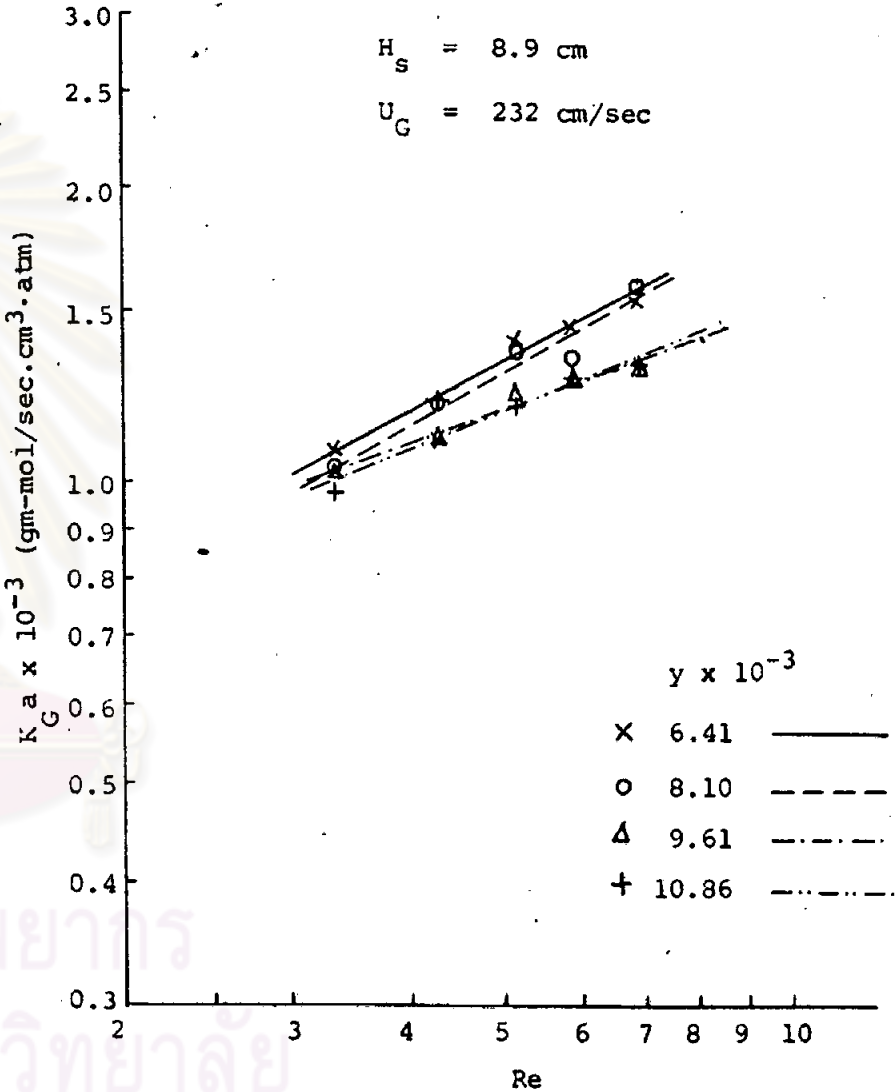

Fig.4.19 Variation of $K_G a$ with Re_L at H_s = 8.9

U_G = 232 cm/sec

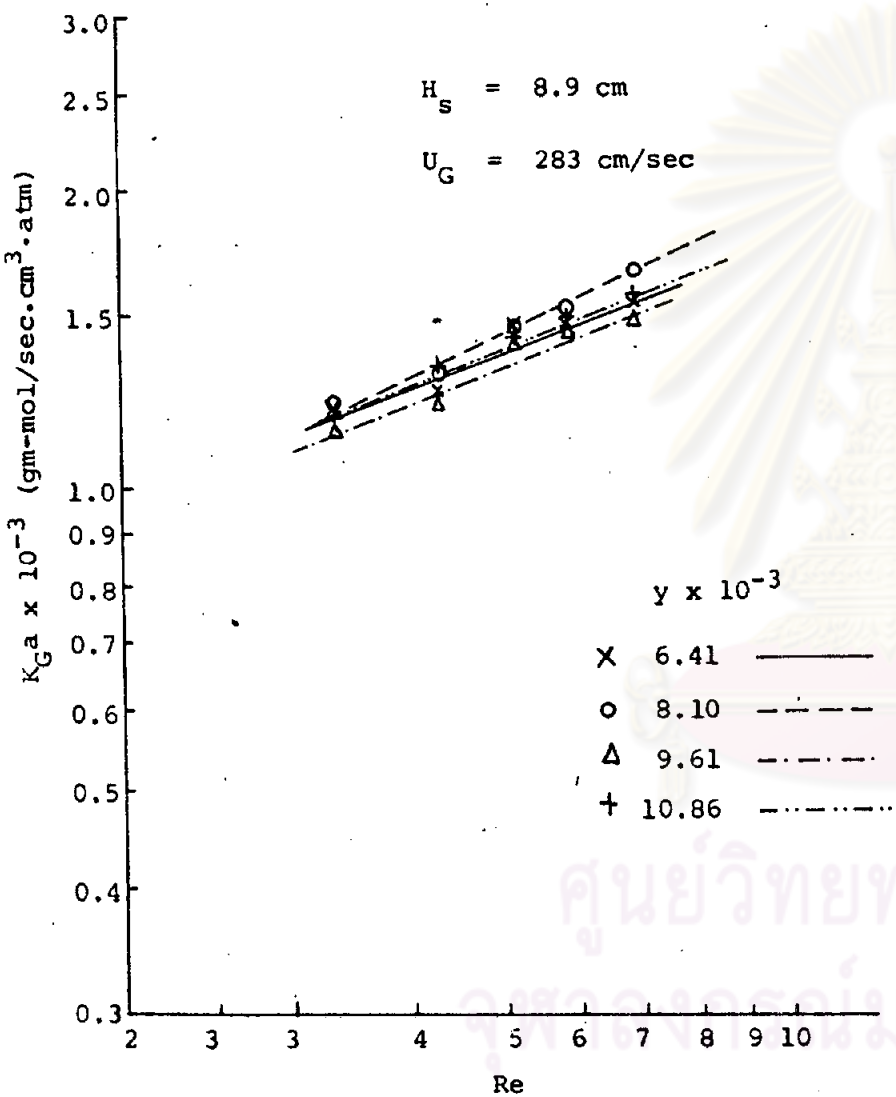

Fig.4.20 Variation of K_Ga with Re_L at H_s = 8.9 cm, U_G = 283 cm/sec

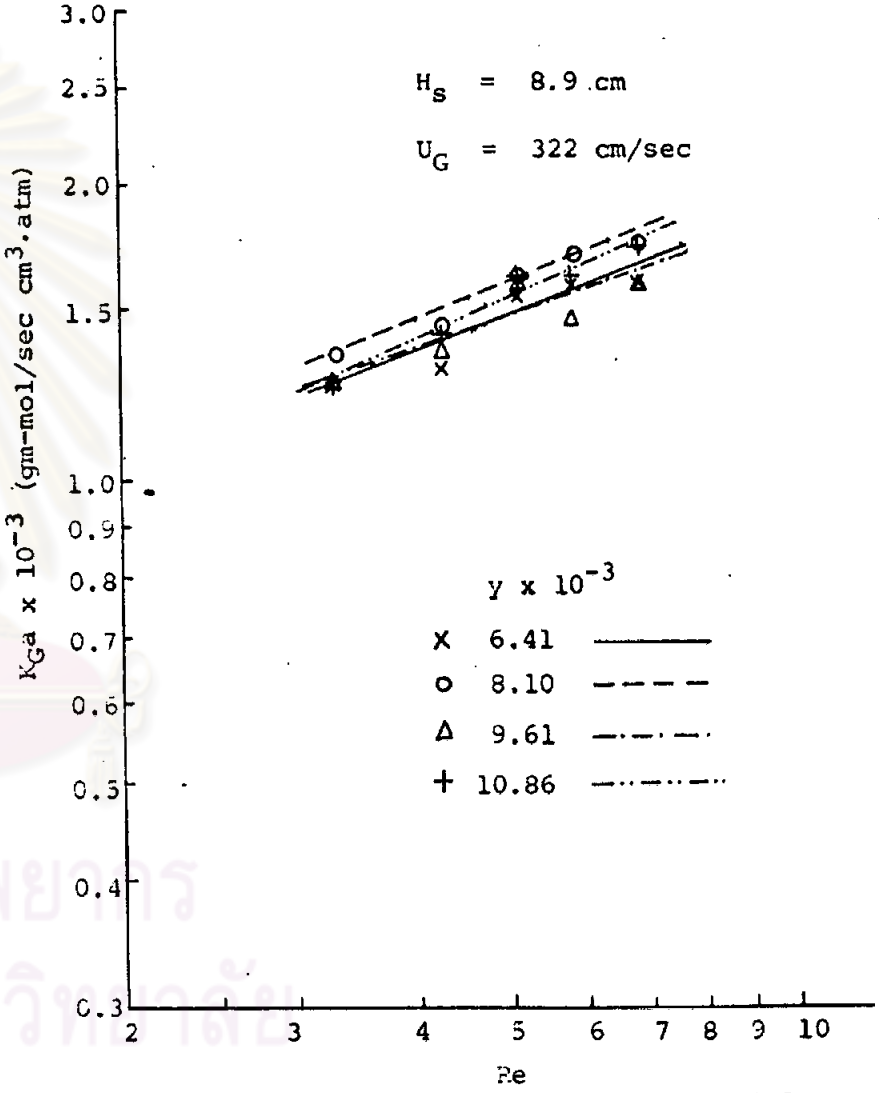

Fig.4.21 Variation of K_Ga with Re_L = 8.9 cm, U_G = 322 cm/sec

were calculated and the average value of the slope was 0.442.

4.2.3 Effects of Bed Heights on Mass Transfer Coefficient ($K_G a$)

Three values of bed height were used and the values of $\frac{D_c}{H_S}$ were calculated and plotted with $K_G a$. The results were shown in Table C-15, C-16, C-17 and plotted in Figure 4.22-4.32. It was observed that $K_G a$ increased with increasing $\frac{D_c}{H_S}$ that is $K_G a$ decreased with increasing bed height. The slope of the lines were calculated and the average value of the slope was 0.621.

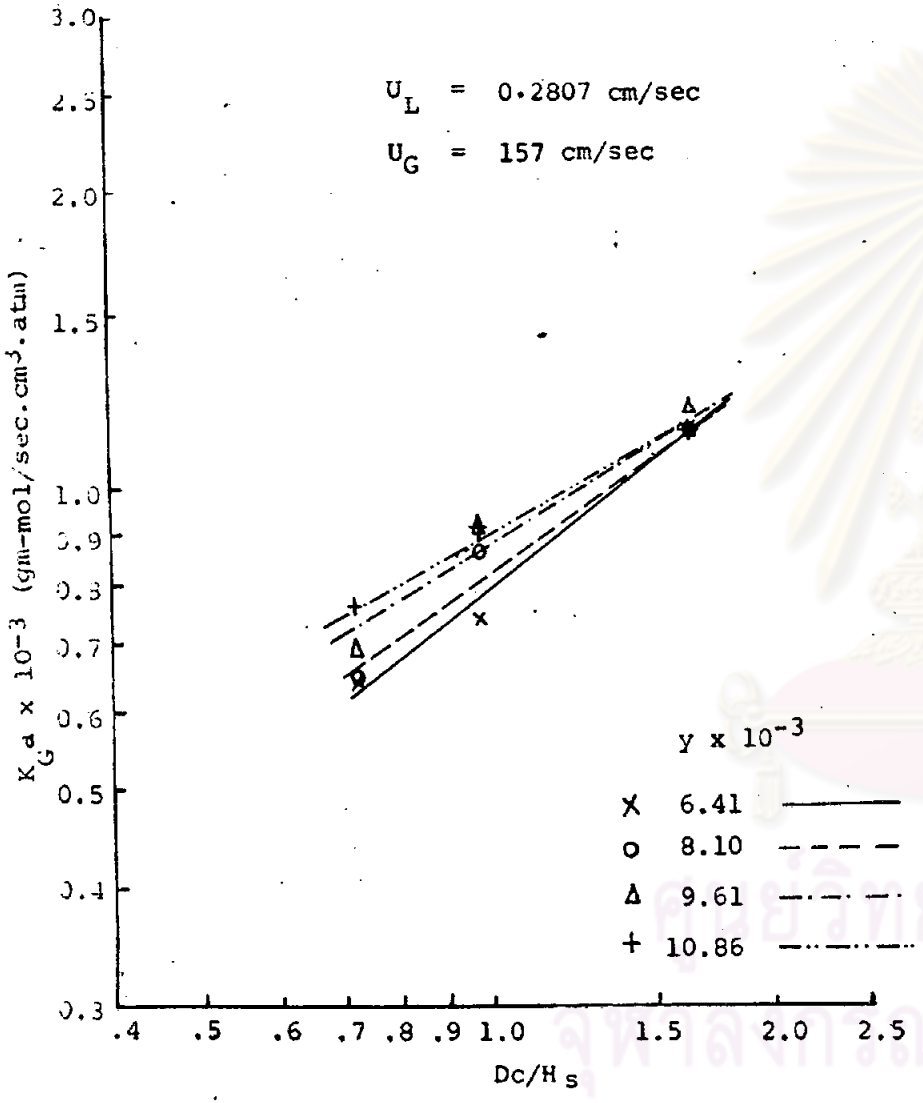

Fig.4.22 Variation of $K_G a$ with $\frac{D_c}{H_s}$ at U_L = 0.2807 cm/sec
U_G = 157 cm/sec

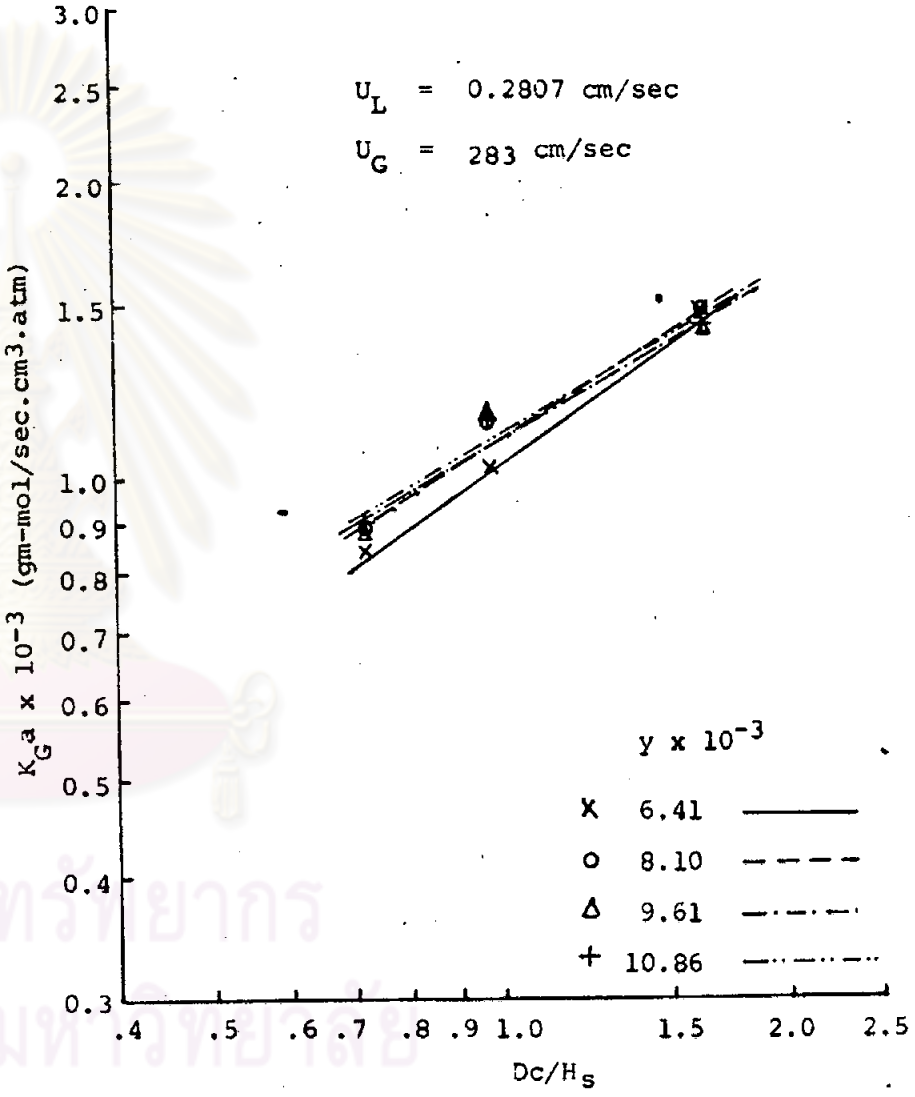

Fig.4.23 Variation of $K_G a$ with $\frac{Dc}{Hs}$ at U_L = 0.2807 cm/sec
U_G = 283 cm/sec

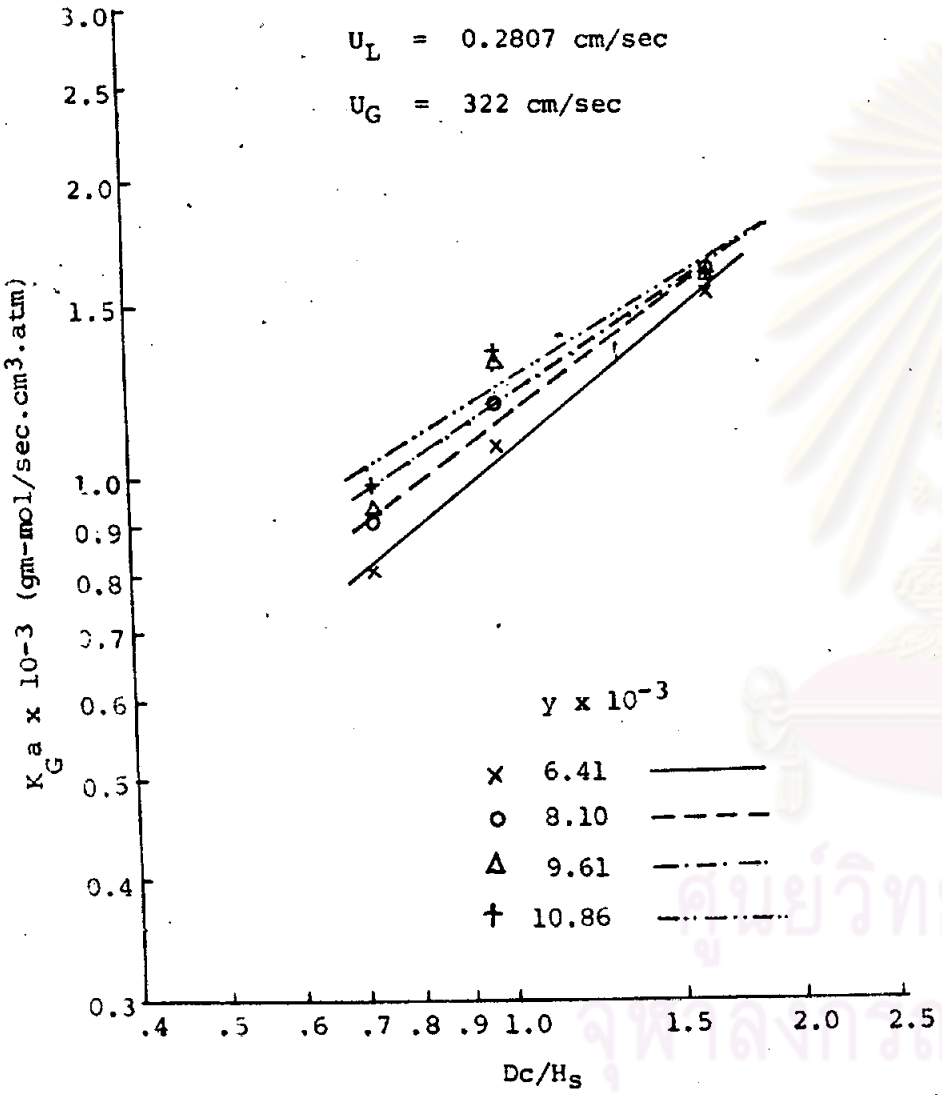

Fig.4.24 Variation of $K_G a$ with $\frac{Dc}{Hs}$ at U_L = 0.2807 cm/sec
U_G = 322 cm/sec

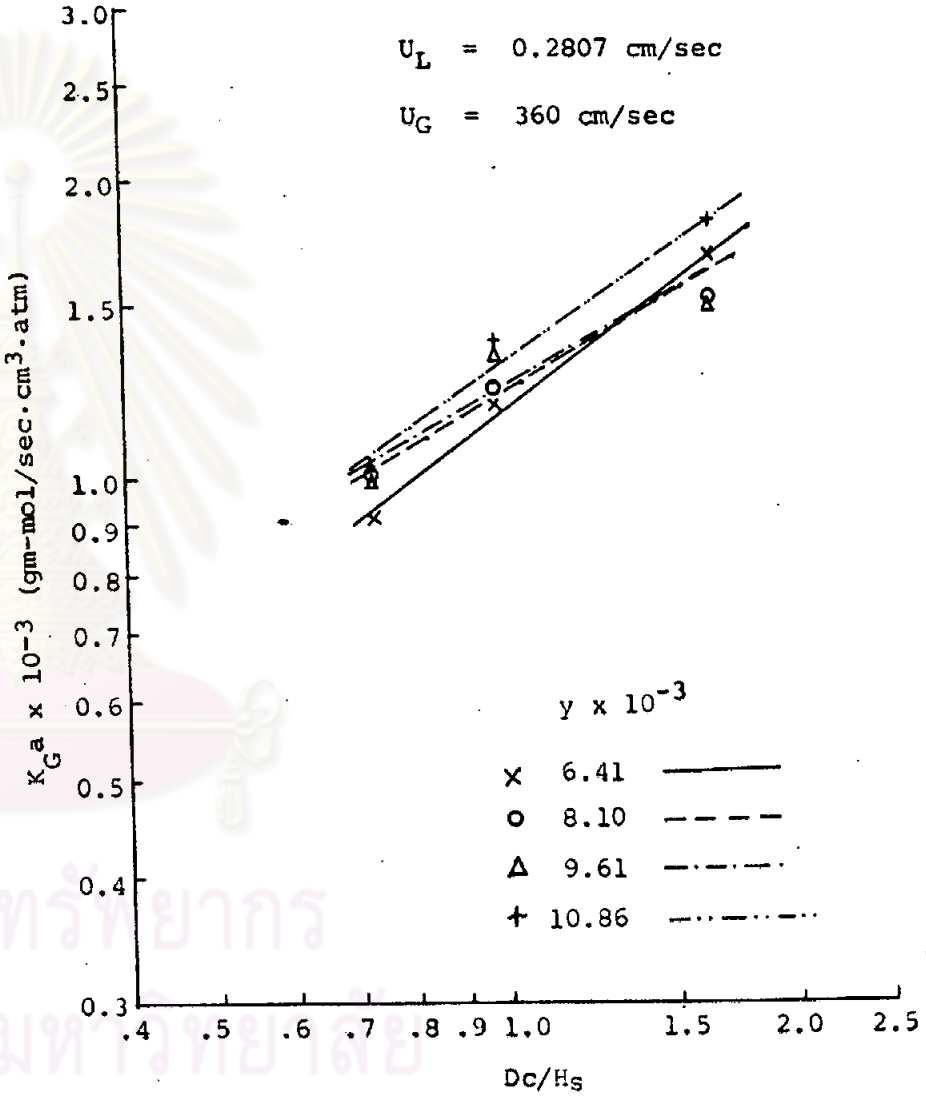

Fig.4.25 Variation of $K_G a$ with $\frac{Dc}{Hs}$ at U_L = 0.2807 cm/s
U_G = 360 cm/sec

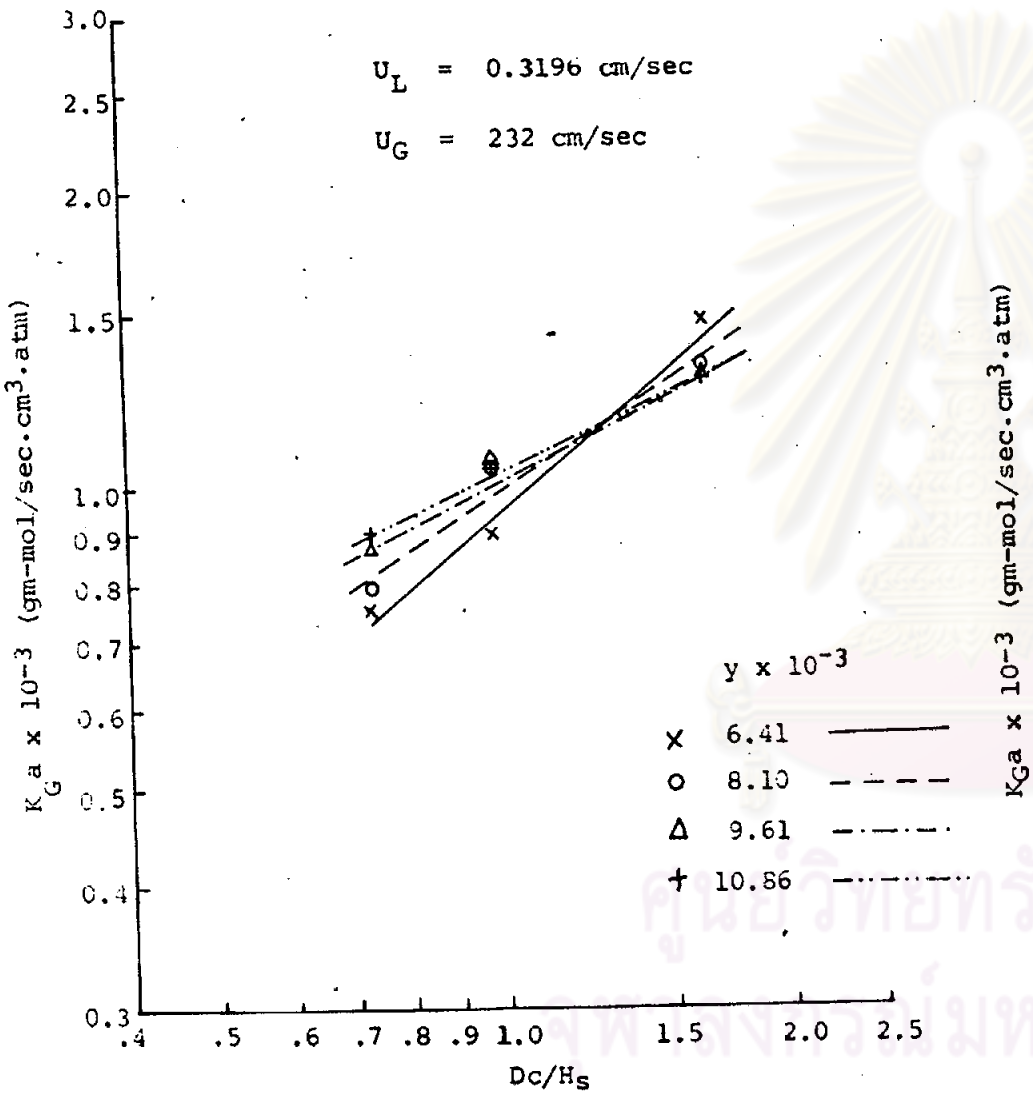

Fig.4.26 Variation of $K_G a$ with $\frac{Dc}{H_s}$ at U_L = 0.3196 cm/sec
U_G = 232 cm/sec

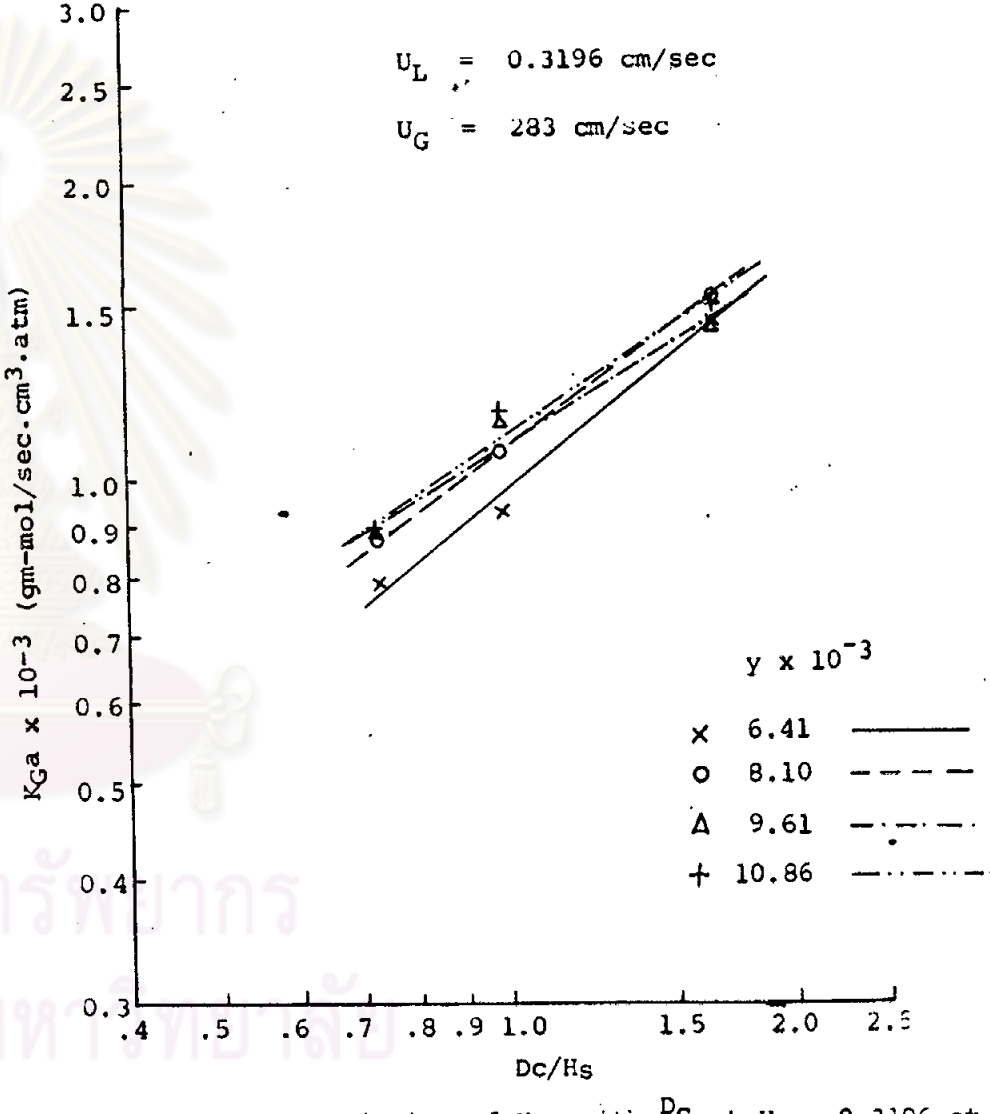

Fig.4.27 Variation of $K_G a$ with $\frac{Dc}{H_s}$ at U_L = 0.3196 cm/
U_G = 283 cm/sec

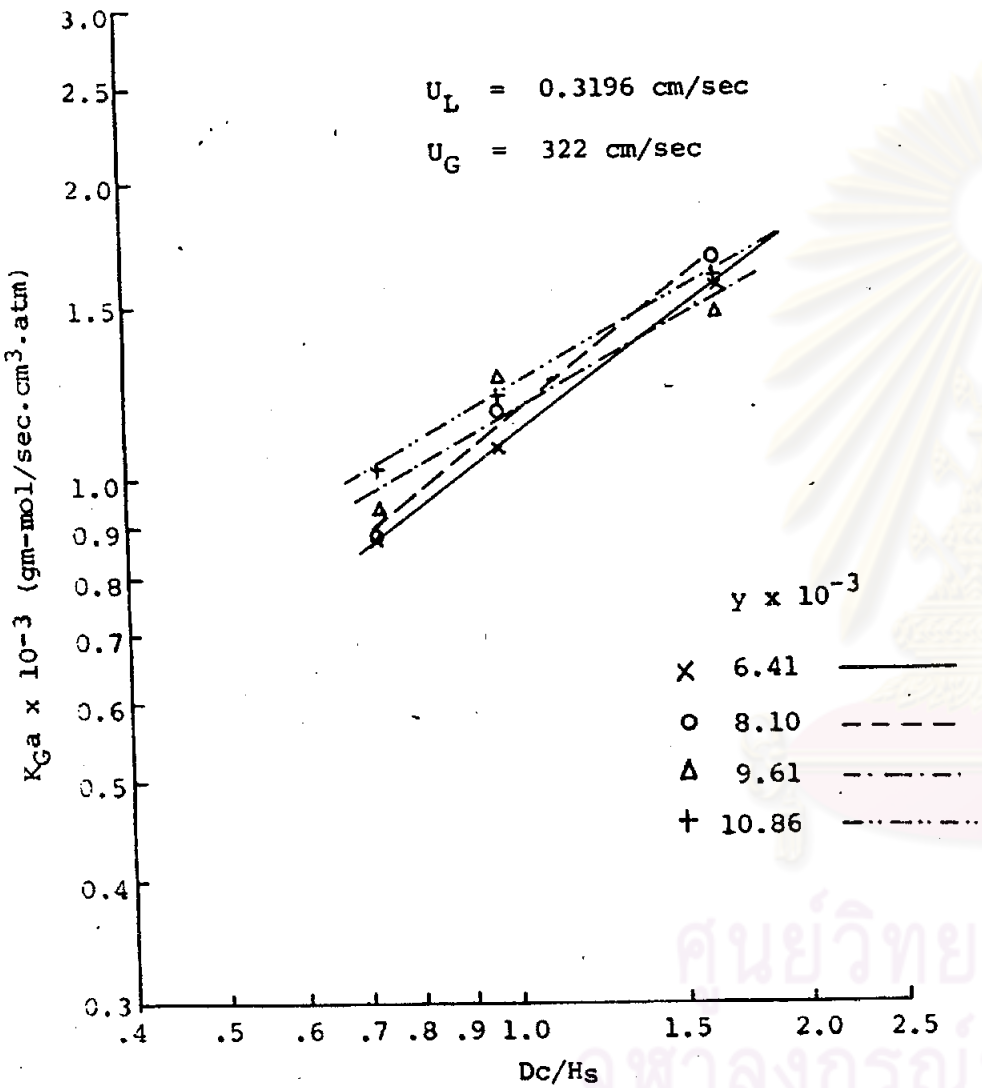

Fig.4.28 Variation of K_Ga with $\frac{Dc}{Hs}$ at U_L = 0.3196 cm/sec
U_G = 322 cm/sec

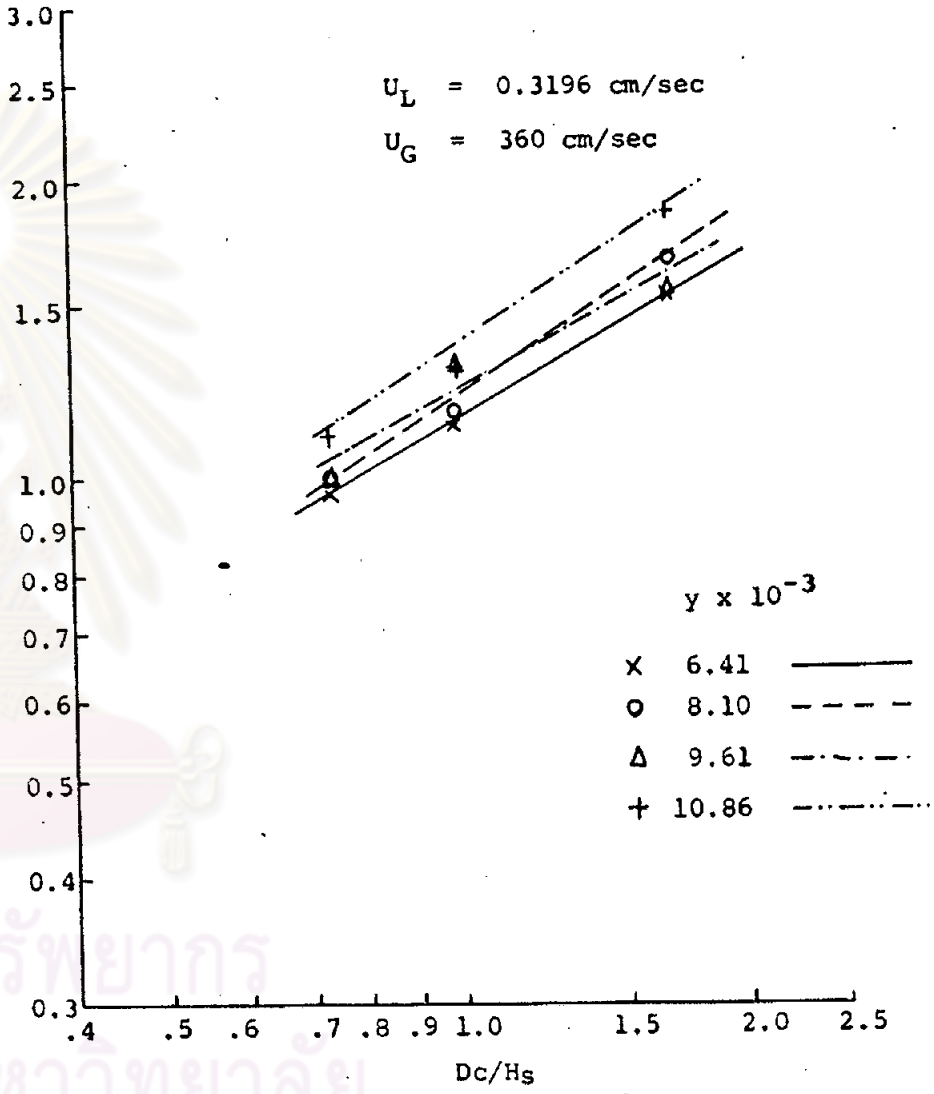

Fig.4.29 Variation of K_Ga with $\frac{Dc}{Hs}$ at U_L = 0.3196 cm/s
U_G = 360 cm/sec

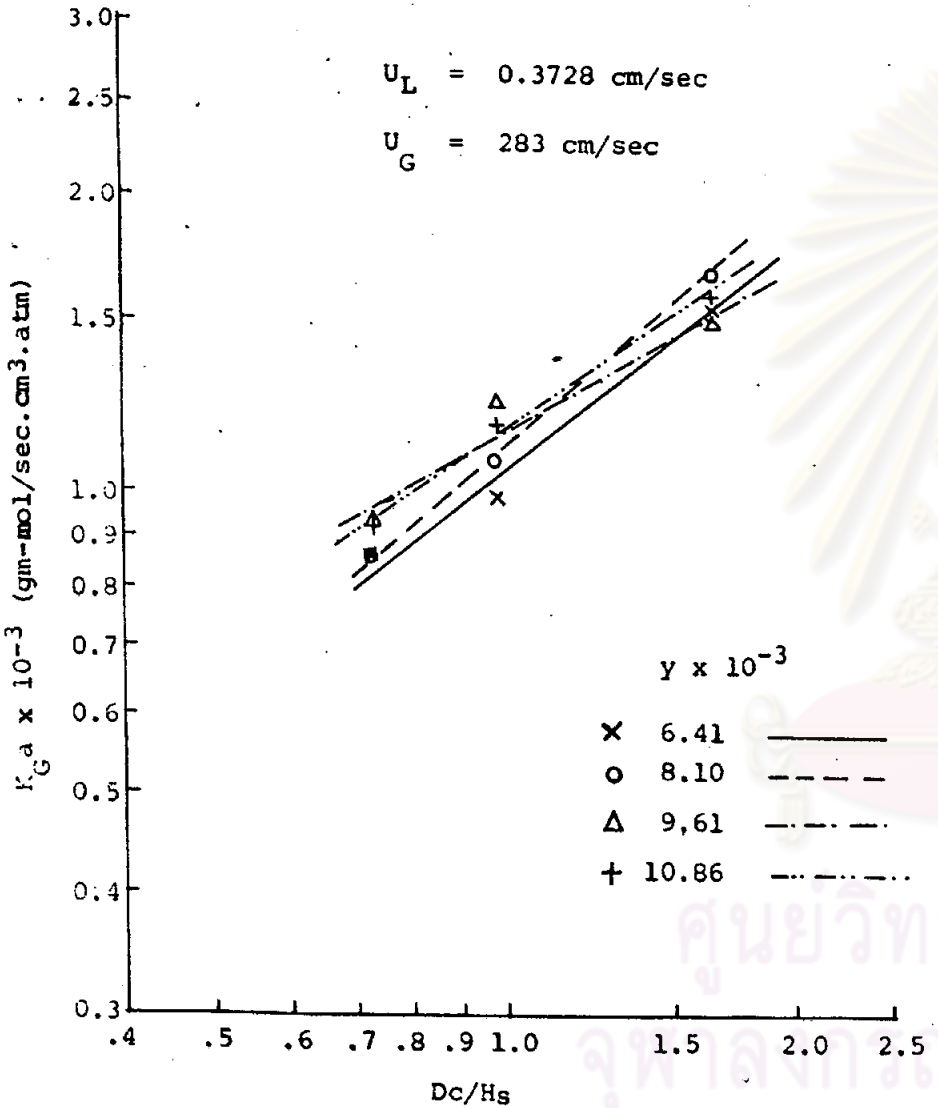

Fig.4.30 Variation of $K_G a$ with $\frac{Dc}{Hs}$ at U_L = 0.3728 cm/sec
U_G = 283 cm/sec

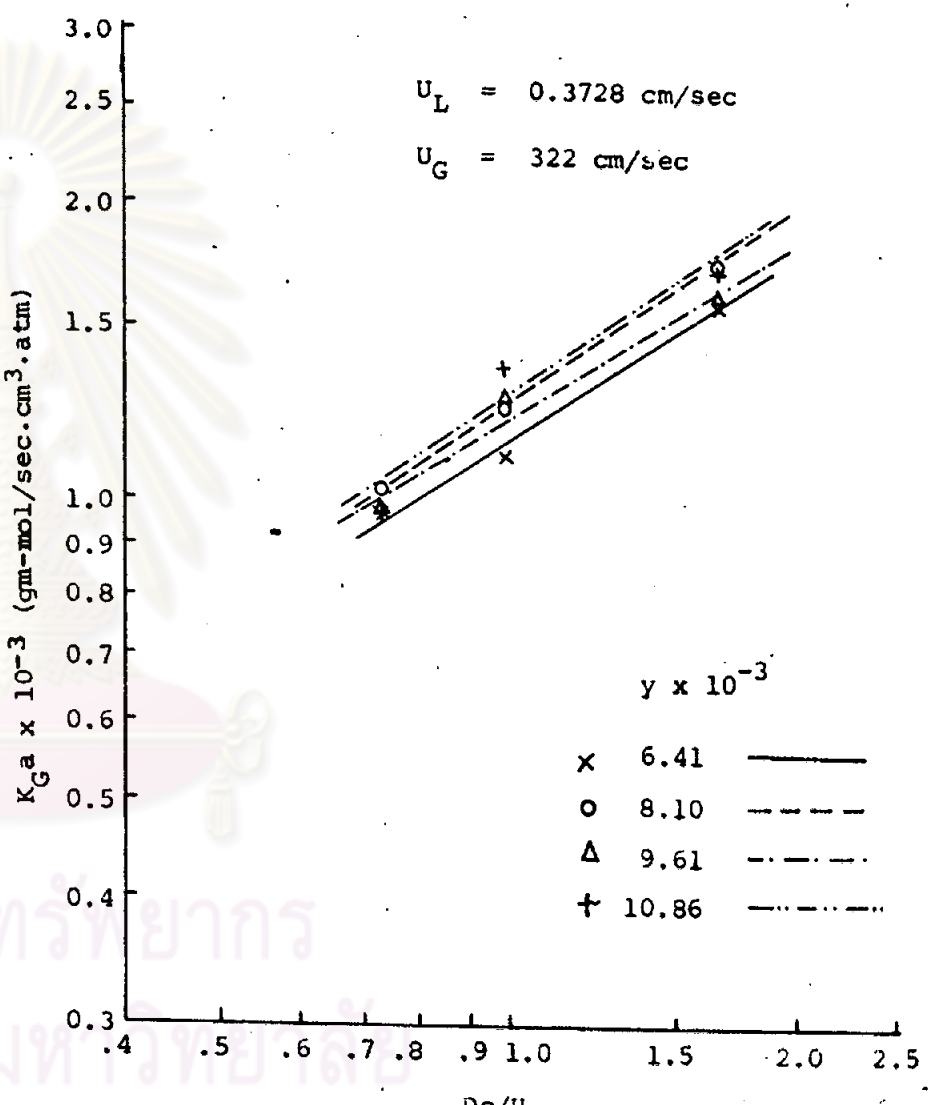

Fig.4.31 Variation of $K_G a$ with $\frac{Dc}{Hs}$ at U_L = 0.3728 cm/sec
U_G = 322 cm/sec

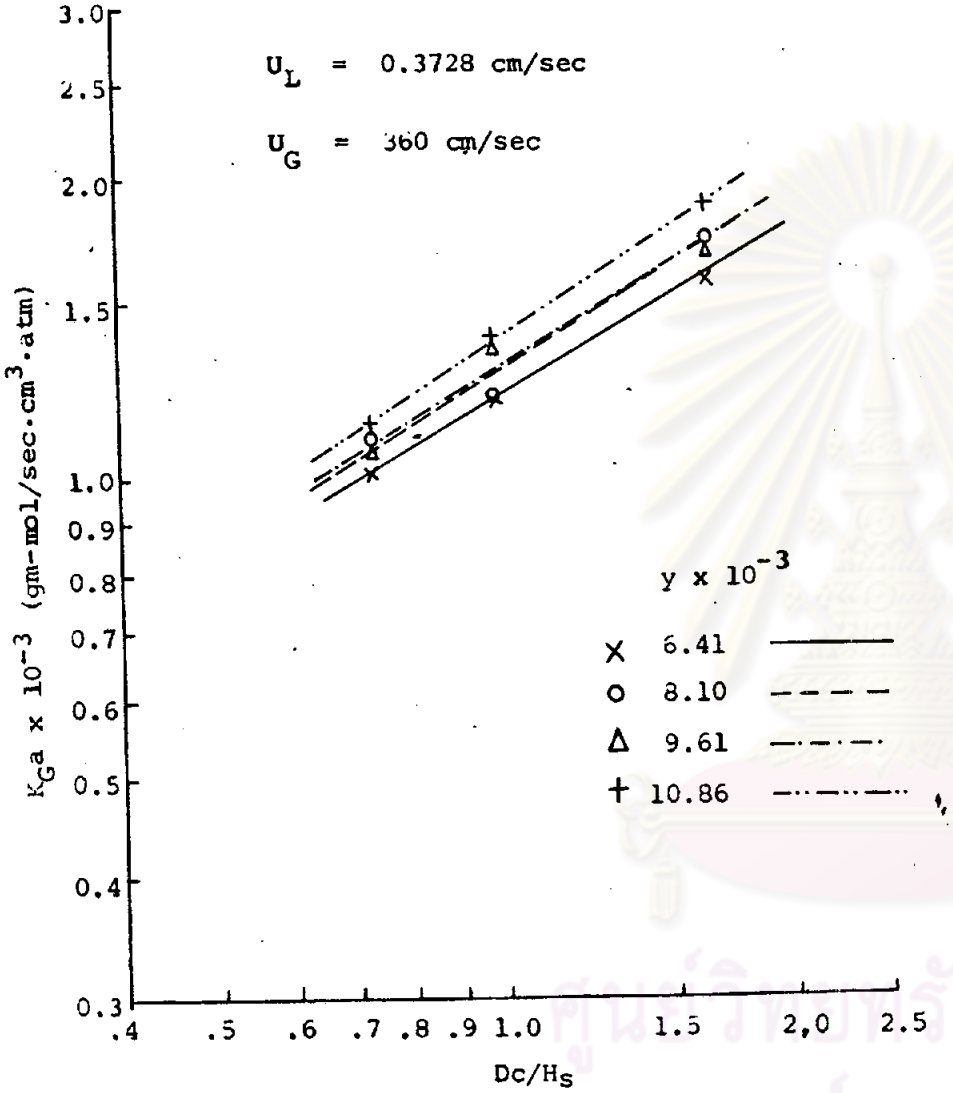

Fig.4.32 Variation of K_Ga with $\frac{Dc}{H_s}$ at U_L = 0.3728 cm/sec

U_G = 360 cm/sec